Isolation and genomic characterization of three PHA degrading bacteria from the marine environment

Degree project presented by Giulia Elli and conducted at Texas A&M University, Corpus Christi

LUNDS UNIVERSITET
Lunds Tekniska Högskola

Supervisor: Mahmoud Sayed Ali Sayed

External supervisor: Dr. Jeffrey Turner
(Texas A&M University, Corpus Christi)

Examiner: Prof. Rajni Hatti-Kaul

Department of Biotechnology

Abstract

The broader goal of this project was to investigate what kind of effects the accumulation of polyhydroxyalkanoates (PHA) in the marine environment might have on the microbial world. Bacteria were isolated from biofilms fouling PHA pellets placed in the sediment-water interface; the goal was to isolate PHA degraders that were also sulphate reducers. Eleven strains were isolated and for three of them genome sequencing and genomic analysis were performed. Two of them (named SRB1LM and SRB3LM) turned out to be *Bacillus* strains and genes involved both in PHA degradation pathways and dissimilatory sulphate reduction pathway were detected in their genomes. These two strains also grew on agar plates where the only carbon source present was PHB (poly-(3-hydroxybutyrate)); they are facultative anaerobes and their growth at 15, 30 and 37°C was studied in laboratory conditions. In a complex medium, they both reached a higher growth rate (μ_{max}) at 37°C; in particular, SRB1LM had the highest μ at 37°C in anaerobic conditions (0.407 h^{-1}), while SRB3LM had the highest μ at 37°C in aerobic conditions (0.849 h^{-1}). The third bacterial genome sequenced belonged to the *Exiguobacterium* genus, whose known species and strains have been isolated from a variety of environments. This isolate (named SRB7LM) can also grow on PHB agar plates, it is a facultative anaerobe but does not have genes of the dissimilatory pathway of sulphate reduction. SRB7LM had a similar μ at the three tested temperatures in anaerobic conditions (0.2 $h^{-1)}$, which were higher compared to the ones in aerobic conditions.

The two *Bacillus* strains could be interesting for the future since the increase in PHA production will cause a higher accumulation in the marine environment; this, coupled with the already high concentration of sulphate, could arise favoring conditions for their growth.

Preface

This degree project was conducted at Texas A&M University Corpus Christi (TAMUCC), Texas, in the Laboratory for Microbial and Environmental Genomics. Supervisor at TAMUCC was Dr. Jeffrey Turner, who is an Assistant Professor of Marine Biology at the University. Day to day work was done in collaboration with Lee Pinnell, a PhD student in Dr. Turner's lab. At Lund University the project was under the supervision of Mahmoud Sayed Ali Sayed and the examination of Prof. Rajni Hatti-Kaul.

First I would like to thank Prof. Rajni Hatti-Kaul and Mahmoud Sayed Ali Sayed who kindly agreed to be my examiner and internal supervisor.

I also kindly thank Dr. Jeffrey Turner for allowing me to be part of this project and for always being supportive throughout my stay in Texas.

A special thanks goes to Lee Pinnell, who let me work independently in the lab but was always there whenever I needed help. It was a pleasure to work on this project with you and to learn many things on the way.

I would like to mention all the students in Dr. Turner's lab, who welcomed me warmly and were always ready to help.

I would like to acknowledge Prof. Daniele Provenzano, he was the one that set everything in motion for my stay in Texas and I will always be grateful for that.

A big acknowledgment goes to the Crafoord Foundation, which awarded me with a travel grant that favored my stay in Texas.

Last but not least, a special thanks goes to my family for always supporting me throughout my studies. I will never forget what you have done and keep doing for me.

Table of Contents

Introduction

Since the mass production of plastic began in the 1940s, it is estimated that 8.3 billion metric tons (Mt) have been produced (Geyer et al., 2017). Of this, only 9% has been recycled, while the rest has either been incinerated (12%) or discarded to landfill (79%). Traditional plastics are derived from fossil hydrocarbons, and due to their chemical composition, most plastics are not biodegradable. Worldwide an estimated 4 to 12 million metric tons of plastic enters the oceans every year (Geyer et al., 2017). Studies have shown that large numbers of marine organisms ingest different types of plastic, and that plastic debris is transferred with marine food webs (Setälä et al., 2014). Coastal ecosystems are particularly susceptible to plastic loading due to their proximity to urban centers (Barnes et al., 2009).

To address the problem of plastic loading, the potential of replacing petroleum-based plastics with bioplastics is being explored. Bioplastics is a broad term describing both bio-based plastics and biodegradable plastics. The main difference between these two categories is that bio-based plastics are polymers obtained entirely or partly from biomass, which typically comes from plants. On the other hand, biodegradable plastics are polymers that can be degraded by microorganisms in the environment. In Figure S1 in the Appendix it is shown how these two categories do not necessarily overlap. For example, polyhydroxyalkanoates (PHA) are a group of biodegradable plastics (European bioplastics, 2019) that are both synthesized and degraded by a diverse lineage of microorganisms.

Partially due to their potential to reduce plastic loading in marine environments, PHAs are considered promising candidates to replace petroleum-based plastic. PHAs are a group of biopolymers produced by microorganisms that have similar properties to petroleum-based plastic (Figure 1). These biopolymers are produced by microorganisms when carbon is abundant but other nutrients such as nitrogen, oxygen, sulphur and phosphorus are limited (Reddy et al., 2017). One of the most abundant PHAs is poly-(3-hydroxybutyrate) (PHB),

which is synthesized by a wide range of bacteria that store it in intracellular granules. For example, members of *Bacillus*, *Pseudomonas* and *Acinetobacter* produce PHB intracellularly (Nehra et al., 2015; Hoseinabadi et al., 2015). Interestingly, these bacteria were isolated from a variety of different environments, ranging from soil to water. Because of their vast potential, the production of biopolymers is expected to increase greatly. For instance, PHA production is expected to increase 10-fold in the next five years (Aeschelmann and Carus, 2015; Keskin et al., 2017). While PHA production is still more expensive compared to petroleum-based plastics, intense research is underway to find a cheaper production method (Tan et al., 2014).

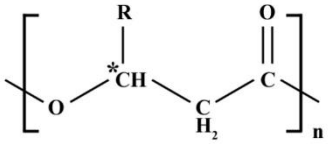

Poly(3-hydroxyalkanoate)

R group	Carbon no.	PHA polymer
methyl	C_4	Poly(3-hydroxybutyrate)
ethyl	C_5	Poly(3-hydroxyvalerate)
propyl	C_6	Poly(3-hydroxyhexanoate)
butyl	C_7	Poly(3-hydroxyheptanoate)
pentyl	C_8	Poly(3-hydroxyoctanoate)
hexyl	C_9	Poly(3-hydroxynonanoate)
heptyl	C_{10}	Poly(3-hydroxydecanoate)
octyl	C_{11}	Poly(3-hydroxyundecanoate)
nonyl	C_{12}	Poly(3-hydroxydodecanoate)
decyl	C_{13}	Poly(3-hydroxytridecanoate)
undecyl	C_{14}	Poly(3-hydroxytetradecanoate)
dodecyl	C_{15}	Poly(3-hydroxypentadecanoate)
tridecyl	C_{16}	Poly(3-hydroxyhexadecanoate)

Figure 1: General chemical structure of poly(3-hydroxyalkanoate). Depending on what R group is present, the PHA polymer differs. Figure taken from (Tan et al., 2014).

Despite the predicted increase in production, little is known about what effects these bioplastics might have on the marine microbial environment. Previous research in our lab demonstrated that PHA pellets were being degraded by the microbial community, and experienced a mass loss of 51% following 424 days of exposure at the sediment-water interface (Pinnell et al., submitted). Extracellular depolymerase enzymes are the enzymes

responsible for the biodegradation of PHA (Mabrouk and Sabry, 2001; Vigneswari et al., 2015) and a 20-fold enrichment of the gene of polyhydroxybutyrate depolymerase was observed in the DNA isolated from PHA-associated biofilm versus both plastic and ceramic biofilms staged at the sediment-water interface (Pinnell and Turner, 2019) . These findings indicate that PHA pellets are being biodegraded in the marine environment by microorganisms that can produce polyhydroxybutyrate depolymerases.

In addition to an increase in depolymerases, previous research in our lab also demonstrated an enrichment of sulphate reducing microorganisms (SRM) in the biofilms formed on PHA pellets versus plastic and ceramic pellets staged at the sediment-water interface (Pinnell and Turner, 2019). SRM are microorganisms capable of reducing sulphate (SO_4^{2-}) into sulfide (S^{2-}) under anaerobic conditions (Jonkers et al., 2005). There are two different biological pathways that microorganisms use: assimilatory and dissimilatory (Grein et al., 2013). In the assimilatory pathway, sulphate is reduced to sulfide in small amounts, and cysteine is produced from it. Cysteine is then used as a building block for a sulphur-containing molecules in the cell. In the dissimilatory pathway, SRM reduce sulphate into large quantities of sulfide, using sulphate as the terminal electron acceptor. As shown in Figure 2, the two pathways have the same first step, where sulphate is activated by reacting with ATP to form adenosine-5'-phosphosulfate (APS) (Taguchi et al., 2004; Ullrich, 2001). After this first step, however, the two pathways use different and specific enzymes to obtain sulphide and cysteine in the assimilatory pathway.

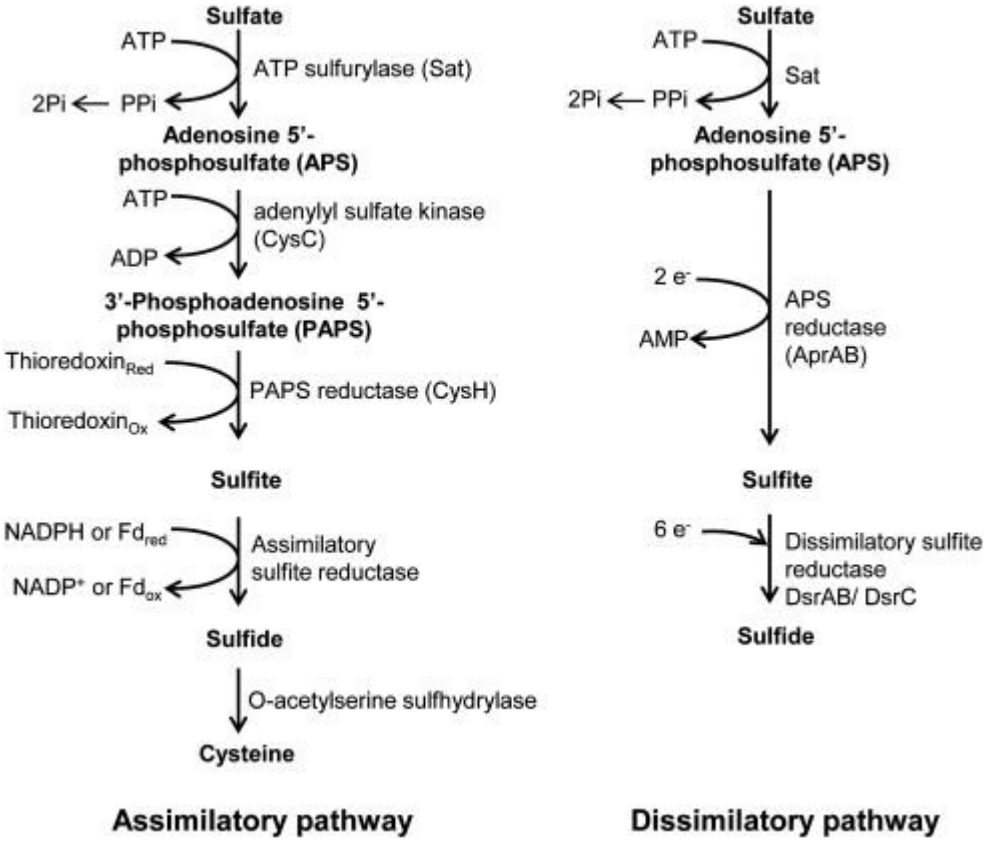

Figure 2: The prokaryotic assimilatory and dissimilatory pathways of sulphate reduction (taken from Grein et al., 2013).

SRM are comprised of a diverse group of microorganisms. They are broadly divided into four different groups (Castro et al., 2002): 1) Gram-negative mesophilic SRB, 2) Gram-positive spore forming SRB, 3) thermophilic bacterial SRB, and 4) thermophilic archaeal SRB. A large proportion of SRM are classified as Deltaproteobacteria (Rabus et al., 2015). This taxonomic class includes many different orders, such as *Desulfovibrionales, Desulfobacterales, Desulfarculales* and *Syntrophobacterales*, that are capable of reducing sulphate. Interestingly, the Gram-positive spore forming SRM contain the only known SRM capable of producing heat-resistant endospores, a feature which is shared with many *Bacillus* and *Clostridium* species (Castro et al., 2002). Though there is no evidence in the literature that members of *Bacillus* are able to use sulphate as electron acceptor, this genus can use nitrite as an electron acceptor in addition to oxygen (Cruz Ramos et al., 2000; Hoffmann et al., 1998). Importantly, previous research demonstrated that a specific SRB (*Desulfotomaculum* sp) was capable of degrading PHB under anaerobic laboratory conditions (Çetin, 2009).

This study utilized microbiological culturing and whole-genome sequencing to isolate and characterize PHA degrading microorganisms from the biofilm formed on PHA pellets. In particular, we attempted to isolate SRM capable of degrading the PHA pellets. Due to the complex nature of microbial biofilms, determining the optimal isolation conditions was the main challenge of this project and different isolation procedures were tested. We hypothesized that SRM capable of degrading PHA would be isolated from the microbial biofilms formed on PHA pellets at the sediment-water interface.

Materials and methods

List of chemicals used

Table 1: List of all chemicals used.

Compound name	Manufacturer
K_2HPO_4	Fisher Scientific, Fair Lawn, NJ, USA
KH_2PO_4	Fisher Scientific
P(3HB)	Sigma-Aldrich, St Louis, MO, USA
NH_4Cl	Fisher Scientific
$(NH_4)_2SO_4$	Fisher Scientific
NH_4NO_3	Fisher Scientific
$(NH_4)_2HPO_4$	LabChem, Zelienople, PA, USA
$(NH_2)_2CO$	Fisher Scientific
$MgSO_4$	Fisher Scientific
$C_6H_8FeNO_7$	Fisher Scientific
$CaCl_2$	Fisher Scientific
$(CH_3COONa)_2*6H_2O$	Fisher Scientific
SRB	Sigma-Aldrich
$Na_2S_2O_3$	Sigma-Aldrich
LB powder	Fisher Scientific
Oxyrase for Agar	Oxyrase Inc., Mansfield, OH, USA
Oxyrase for Broth	Oxyrase Inc.

Sample deployment and collection

PHA pellets were deployed at the sediment-water interface of the Upper Laguna Madre, Texas in microcosms as described previously (Pinnell & Turner 2019). Briefly, 5.0 g of PHA pellets (Doctors Foster and Smith, Rhinelander, WI, USA) were deployed inside custom made microbial capsules at the sediment-water interface from September 20, 2018 to May 8, 2019. Pellets were approximately 3-4 mm in diameter and therefore were considered microplastics (Andrady 2011). The capsules utilized 315 µm Nitex mesh to contain the pellets and permit the exchange of water, nutrients, bacteria, and some grazers, but limit

the entry of larger organisms. All pellets were processed within two hours of collection. Prior to isolation, pellets were washed three times with 0.22 µm filter-sterilized, site-specific seawater to remove any organisms not part of the biofilm.

Growth media

MSM-P(3HB) liquid medium. Minimal salts medium (MSM) containing PHB as sole carbon source was used as described previously (Vigneswari et al., 2015). Briefly, the medium contained the following compounds: 2.56 g/L of K_2HPO_4, 2.08 g/L of KH_2PO_4 , 7.5 g/L of P(3HB) , and 1 g/L of one of the following nitrogen sources: NH_4Cl , $(NH_4)_2SO_4$, NH_4NO_3 , $(NH_4)_2HPO_4$ and $(NH_2)_2CO$. The medium was then autoclaved at 121°C and 15 psi for 15 minutes. At inoculation, filter sterilized $MgSO_4$ (0.5 g/L), $C_6H_8FeNO_7$ (500 µg/L), $CaCl_2$ (0.1 µg/L) and $(CH_3COONa)_2*6H_2O$ (0.2 g/L; pH 6) were added.

Sulphate reducing medium. SRM were isolated using sulphate reducing broth (SRB). Two variations of SRB were used: 1) 'SRB +', which included 10 g/L of sodium thiosulfate ($Na_2S_2O_3$) added to the medium, and 2) 'SRB–', which was just the stock SRB. Liquid medium was prepared by boiling to dissolve the medium then sterilized by autoclaving at 121°C and 15 psi for 15 minutes. Solid medium was prepared by the addition of 1.5% Difco Agar (BD, Franklin Lakes, NJ, USA).

Lysogeny broth (LB) medium. 25 g of LB powder (Fisher Scientific) was dissolved in 1 liter of distilled water and sterilized by autoclaving at 124°C, 19 psi for 15 minutes.

Overlay plates (SRB plates): 1 mL of Oxyrase for Agar was added to 19 mL of medium (containing 1.5% of Agar) when it was still liquid; the inoculum (100 µL) was added to this mixture and then the medium was poured into sterile agar plates. After it solidified, 5 mL of medium supplemented with 250 µL of Oxyrase was added as an overlay. Plates were then sealed with parafilm and incubated.

Isolation of PHA biofilm community members

Members of the PHA biofilm capable of growing in SRB and PHB media were isolated following the exposure in two different procedures. One procedure involved adding PHA

pellets to either SRB+ or SRB- liquid medium, while for the other procedure PHA pellets were added to MSM-PHB liquid medium. In the two procedures, PHA pellets collected from the field at three different times were used.

In the first procedure, PHA pellets were collected after 153 days exposure. They were incubated in SRB+ or SRB- medium for 48 hours at 200 rpm, in anaerobic conditions and at three temperatures (27, 32 and 37 °C). To obtain anaerobic conditions, 0.1 mL of Oxyrase for broth was added per 1 mL of medium at inoculation. After 48 hours, cells from SRB- tubes were added to MSM-P(3HB) liquid broth and incubated at the same temperatures and 200 rpm in anaerobic conditions. To obtain anaerobic conditions the liquid was bubbled with N_2 gas (10 minutes) in order to remove all the oxygen, the overhead space was then flushed with N_2 as well to remove oxygen from the air. After 7 days of growth the cells were plated on SRB- plates (overlay plates) and incubated at 32°C. Isolated colonies were collected after 48 hours of incubation.

In the second procedure, PHA pellets were collected after 181 days exposure. They were added to the five MSM-PHB media described previously and incubated at 37°C with 150 rpm horizontal shaking. Anaerobic conditions were also used (liquid was bubbled with N_2 for 10 minutes in the overhead space for 1 minute). After 7 days cells of growth, the cells were plated on overlay plates with SRB- and SRB+ agar and incubated at 37°C. After 72 hours of incubation, single colonies were collected.

Table 2 summarizes the steps involved in the two isolation procedures.

Growth on PHB solid medium

PHB solution. 1 g of PHB powder (Sigma-Aldrich) was added to 100 mL of distilled water. The solution was sonicated for 15 minutes (Branson 2800 Ultrasonic cleaner, Branson Ultrasonics, Danbury, CT, USA) and then autoclaved at 124°C and 19 psi for 30 minutes. The solution was then was added to 900 mL of liquified agar solution (1.5%). Final PHB concentration was 0.1%. When anaerobic conditions were necessary, the solution was bubbled with nitrogen gas for 10 minutes when it was still liquid.

Minimal salt agar medium. Five different MSM solutions were prepared the same way as described above, with one exception that PHB was not added to these solutions. Instead 1.5 g of Difco™ Agar (BD) was added to 100 mL of medium. The media was autoclaved at 124°C, 19 psi for 30 minutes. At inoculation, the same micronutrients as the liquid media were added. When anaerobic conditions were necessary, the solution was bubbled with nitrogen gas for 10 minutes when the medium was still liquid. Agar plates were prepared by pouring 6 mL of the MSM agar as the bottom layer in the plate. The upper layer was formed by adding 4 mL of the PHB solution, which contained PHB as the sole carbon source.
The plate culture technique was done, as previously shown by Mabrouk and Sabry (2001), by first dipping a sterile tooth pick into an actively growing culture, then the tooth pick was punctured into the polymer agar plate. Three conditions were tested: aerobic, anaerobic and aerobic + oxyrase in the medium. For aerobic conditions, after the inoculation the plates were then sealed with parafilm and incubated; for anaerobic conditions, plates were placed in an anaerobic chamber where anaerobic conditions were obtained using the AnaeroPack® System (Mitsubishi Gas Chemical Co., Inc, Tokyo, Japan). All plates were incubated at 37°C for 5-7 days.

Growth rates of isolates

To determine their optimal growth conditions, isolates were grown aerobically and anaerobically in LB broth at three different temperatures: 15, 30, 37 °C, with horizontal shaking at 150 rpm. Their OD_{600} was measured with a BioSpectrometer (Eppendorf AG, Hamburg, Germany) at 1, 2, 4, 6, 8, 12, 24, 30, 36, 48, 60, 72 and 96 hours after inoculation. At time 0 the cells were all diluted to a starting OD of 0.02. Anaerobic conditions were achieved by bubbling the medium with N_2 gas for 10 minutes.

DNA isolation

Genomic DNA was isolated from three isolates (SRB1LM, SRB3LM, and SRB7LM) using the DNeasy UltraClean Microbial kit (Qiagen, Hilden, Germany) following the manufacturer's protocols. The DNA was quantified and assayed for quality (A260/A280) using a BioPhotometer D30 (Eppendorf, Hamburg, Germany) and stored at -20 °C.

Genome sequencing

Genomic library preparation and sequencing was carried out by Molecular Research LP (Shallowater, TX, USA). Libraries were prepared using a Nextera DNA Flex Library Preparation Kit (Illumina, San Diego, CA) and 50 ng of genomic DNA. Final library concentration was measured using the Qubit dsDNA HS Assay Kit (Life Technologies) and the average library size was determined using an Agilent 2100 Bioanalyzer (Agilent Technologies, Santa Clara, CA). Prior to sequencing 700 bp size selection was performed using a BluePippin DNA size selection system (Sage Science, Beverly, MA). DNA was sequenced using an Illumina NovaSeq instrument using paired-end chemistry (2 x 150 bp). The DNA concentrations, the average size of the sequencing libraries, and the number of sequence reads are reported in Table 2.

Genome assembly

Overlapping paired reads were merged using FLASH version 1.2.11 (Magoc and Salzber 2011). Merged reads were trimmed of adapter sequences and low-quality bases with Trim Galore! version 0.4.4, which utilizes Cutadapt (Martin 2011) and FastQC (Andrews 2010). Draft genomes were assembled *de novo* with both Velvet version 1.2.10 (Zerbino and Birney 2008) and SPAdes version 3.11 (Bankevich et al 2012). The optimal k-mer size for velvet assemblies was determined manually by comparing assembly metrics with k-mer sizes ranging from 11 to 111. SPAdes was run using the 'careful' flag and k-mer sizes of 21, 33, 55, and 77. Additionally, MaSuRCA version 3.1.3 (Zimin et l, 2013) was used to *de novo* assemble raw sequence reads. Genome assembly metrics were computed and compared using QUAST version 4.1 (Gurevich et al., 2013) and are reported in Table 3. In all cases, Velvet produced the most contiguous assembly and was selected for further analysis.

Genome analysis

The three isolates were analyzed with the Pathosystems Resource Integration Center's (PATRIC) (Wattam et al 2017) comprehensive genome analysis service. The automated PATRIC service includes annotation with RASTtk (Brettin et al 2015), prediction of nearest neighbors with Mash/MinHash (Ondov et al., 2016), clustering of homologous proteins with OrthoMCL (Enright et al., 2002), alignment of conserved clusters with MUSCLE (Edgar, 2004), trimming with Gblocks (Talavera et al., 2007), and concatenation followed by inference of a ML tree with RAxML (Stamatakis, 2014). Based on the initial tree containing nearest neighbors, all representative genomes within *Bacillus* in the PATRIC database (n=98) were included in the tree for SRB1LM and SRB3LM, and all complete genomes within *Exiguobacterium* (n=75) were included in the tree for SRB7LM.

Additionally, the three isolates were compared to all publicly available bacterial genomes in GenBank (n= 207,806) by average nucleotide identity (ANI) with fastANI (Jain et al 2018), using >95% ANI as the intra-species threshold and <83% as an inter-species threshold.

Additionally, a comparison between known genes involved in PHA degradation pathway and in sulphate reduction pathways and genes in the isolates genomes was performed. First, from each genome assembly, Prodigal was used to predict all the genes from the whole genome (Hyatt et al., 2010). After this first step, the predicted genes sequences were aligned against known genes sequences present in the database. Two separate searches were performed using hmmsearch (Finn et al. 2011), one against known genes involved in the reduction of sulphate into sulfide, the other one against known PHA depolymerases. In order to be a positive match, an E-value of 10^{-5} was set as the threshold.

Results

Isolation of PHA degrading bacteria from marine environment

A total of 11 different bacterial strains were isolated from the biofilms formed on PHA pellets at sediment-water interface. Three different isolation methods were implemented. The PHA pellets were added to liquid media to select for bacteria present in the biofilm capable of using PHB as a sole carbon source or reduce sulphate. Pellets were initially added to MSM-PHB liquid broth or SRB liquid broth. Growth within SRB broth was easy to identify because of the initial clarity of the medium and the opaqueness of subsequent growth (Figure 3).

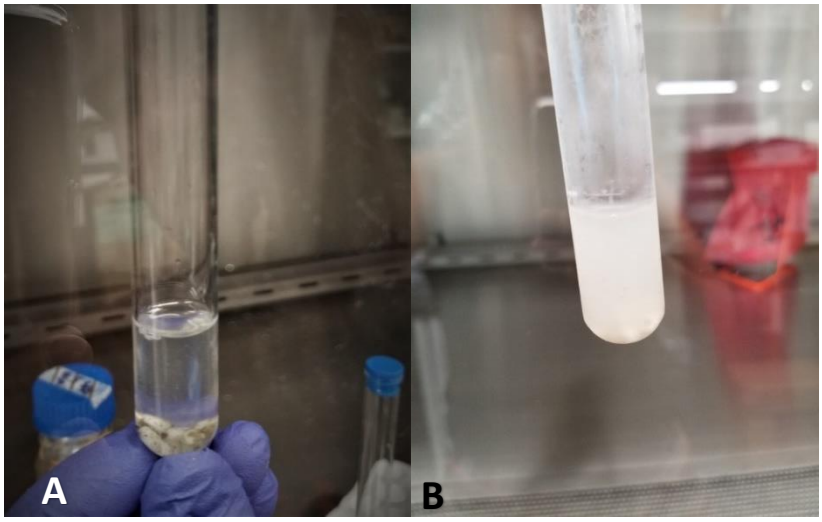

Figure 3: In panel (A), time zero of incubation, SRB liquid broth was the medium used and anaerobic conditions were obtained using Oxyrase. PHA pellets can be seen at the bottom of the tube. In panel (B), the same tube after 2 days of incubation at 30°C, 150 rpm. The change in turbidity and clarity indicates cells growth.

Contrastingly, MSM-PHB liquid medium was initially opaque (Figure 4), and resulting growth was harder to detect. However, a yellowish tint could be detected in some of the tubes, indicating growth.

Figure 4: PHA pellets added to MSM-PHB medium; the presence of PHB gave the medium this white color and poor clarity. PHA pellets cannot be seen but they were present at the bottom of the tube. Picture taken at time 0 of inoculation.

Isolates SRB1LM – SRB6LM were initially incubated in SRB liquid broth, followed by a second incubation in MSM-PHB liquid broth, and then isolated on SRB plates. Isolates SRB7LM, SRB8LM and SRB9LM were cultured first in MSM-PHB liquid broth and then isolated on SRB plates. Finally, SRB10LM and SRB11LM were cultured in SRB liquid broth and then isolated on SRB plates. A picture of each colony was taken, and isolates were selected for genome sequencing based on their morphologies (Figure 5). Isolates with different morphologies were chosen to maximize the odds of sequencing different microorganisms.

Table 2: Summary of the two isolation procedures.

	SRB1-6LM	**SRB7-9LM**
First step	SRB (- or +) for 2 days	MSM-PHB for 7 days
Second step	MSM-PHB for 7 days	SRB + agar plates
Third step	SRB – agar plates	/

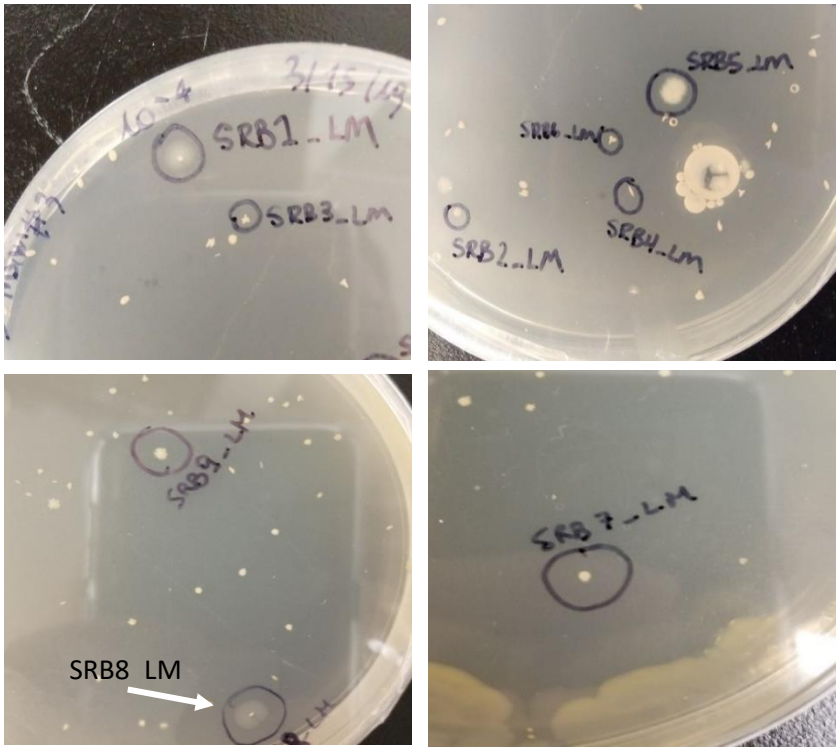

Figure 5: Single colonies formed after two days of incubation at 30°C on SRB agar plates (SRB- agar plates for SRB1LM, SRB2LM, SRB3LM, SRB4LM, SRB5LM, SRB6LM, SRB8LM and SRB9LM; SRB+ agar plates for SRB7LM). The highlighted colonies were isolated.

Growth conditions

To determine their optimal growth conditions, the three isolates selected for genome sequencing were grown aerobically and anaerobically in a complex medium at three different temperatures. The typical range of water temperatures at the sample site fluctuates seasonally from 15 to 35° C, so their growth was tested at 15, 30 and 37°C. The OD_{600} of the cultures was monitored at different time points by measuring the absorbance at 600 nm. Figures 6 thru 8 demonstrate the growth curves of each isolate at the different conditions and temperatures. All three isolates were facultative anaerobic, as they were able to grow both in aerobic and anaerobic conditions. In all cases, a higher OD was obtained when cells grew aerobically. Growth rates were then measured to compare all the different conditions used. To measure the growth rate, the Ln of OD in the exponential phase was plotted against the time (From Figure S5 to Figure S22 in the Appendix); the slope of the line obtained is the maximum growth rate (μ_{max}), which is specific to each isolate and each condition as well. The μ_{max} of each isolate at the different temperatures and both in aerobic and anaerobic conditions was measured and they can be found in Table 3.

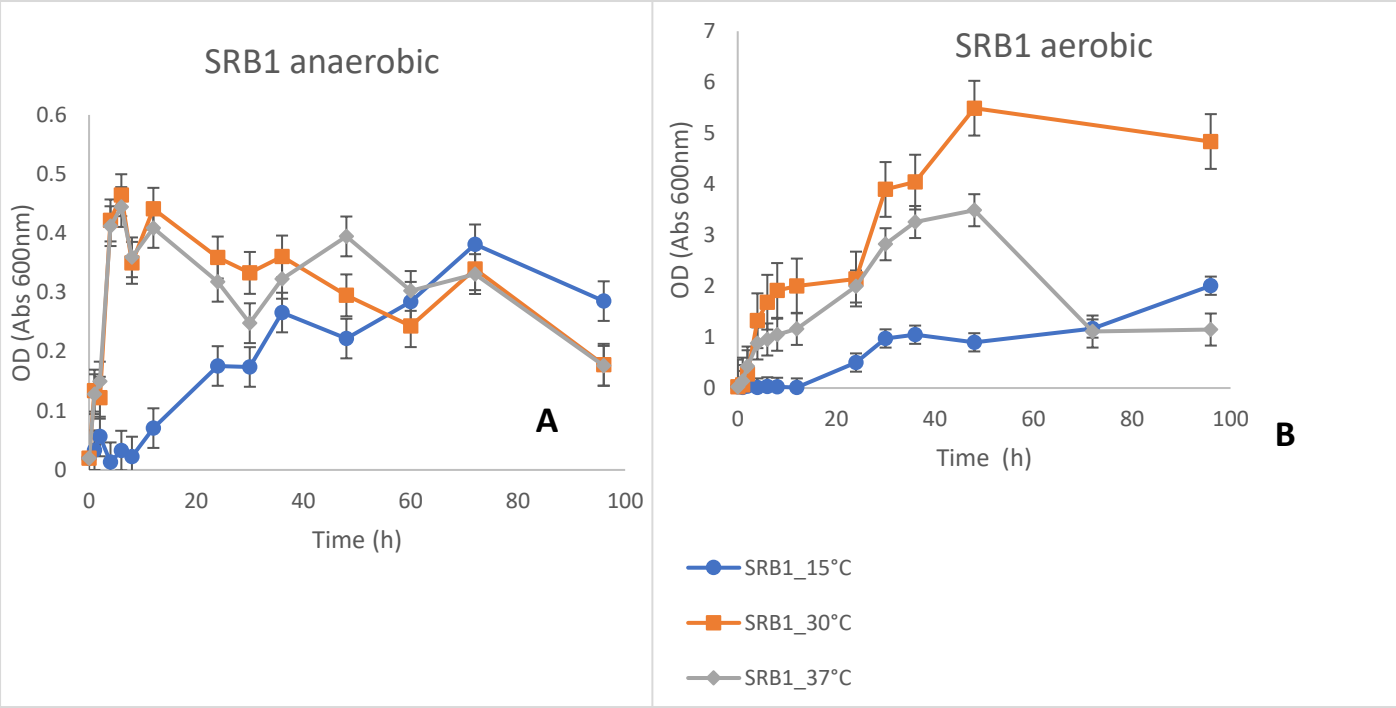

Figure 6: Growth curves of SRB1LM grown on LB medium. (A) cells were grown in anaerobic conditions, (B) cells were grown in aerobic conditions with 150 rpm shaking for 4 days. Each curve represents a growth curve of the isolate grown at a specific temperature (15, 30 or 37°C) and the legend indicates the temperature. On the y-axis OD_{600}, and the x-axis the time in hours is depicted.

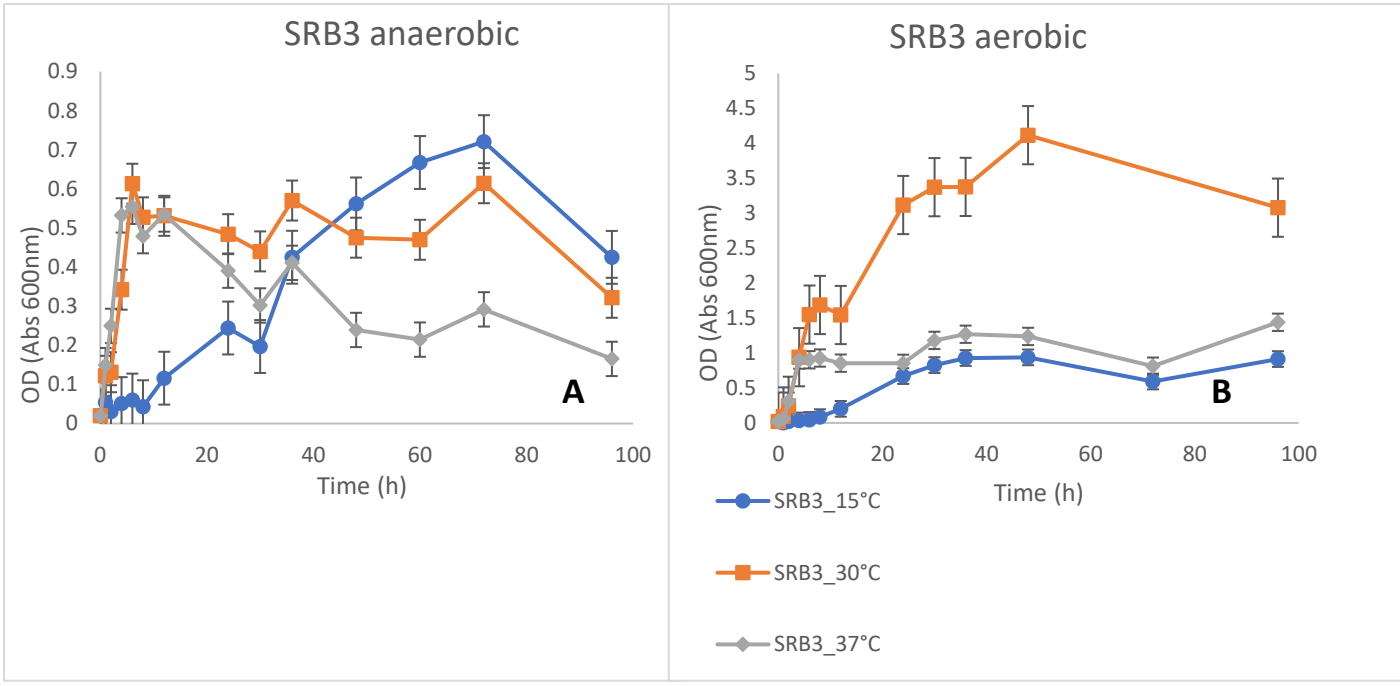

Figure 7: Growth curves of SRB3LM grown on LB medium. (A) cells were grown in anaerobic conditions, (B) cells were grown in aerobic conditions with 150 rpm shaking for 4 days. Each curve represents a growth curve of the isolate grown at a specific temperature (15, 30 or 37°C) and the legend indicates the temperature. On the y-axis OD_{600} is depicted, and on the x-axis the time in hours is depicted.

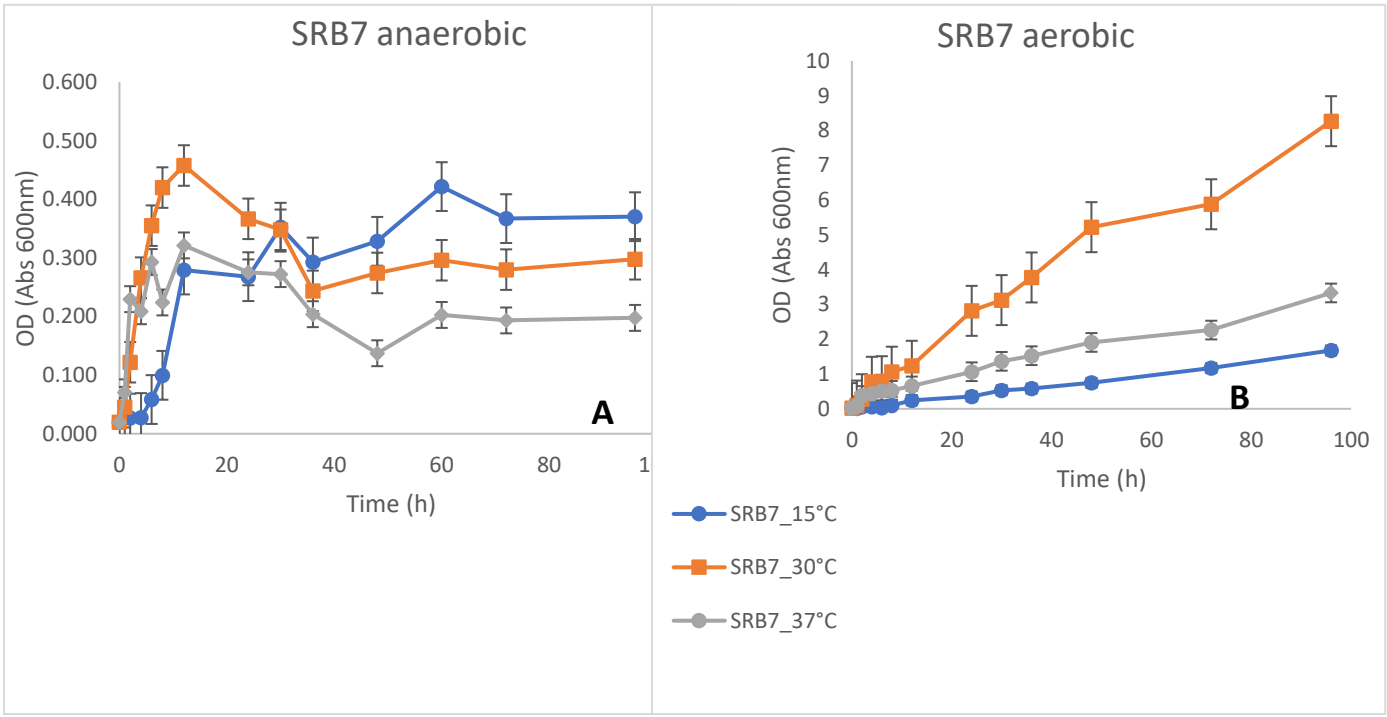

Figure 8: Growth curves of SRB7LM grown on LB medium. (A) cells were grown in anaerobic conditions, (B) cells were grown in aerobic conditions with 150 rpm shaking for 4 days. Each curve

represents a growth curve of the isolate grown at a specific temperature (15, 30 or 37°C) and the legend indicates the temperature. On the y-axis OD_{600}, and on the x-axis the time in hours is depicted.

Table 3: μ_{max} of each isolate at the different conditions tested. The slope of the line obtained by plotting the Ln(OD) (y-axis) and the time (x-axis) represents the μ_{max}.

Conditions	**μ SRB1LM (h^{-1})**	**μ SRB3LM (h^{-1})**	**μ SRB7LM (h^{-1})**
15°C, aerobic	0.111	0.081	0.0257
15°C, anaerobic	0.115	0.044	0.261
30°C, aerobic	0.03	0.314	0.0447
30°C, anaerobic	0.334	0.347	0.2
37°C, aerobic	0.049	0.849	0.0296
37°C, anaerobic	0.407	0.418	0.22

Growth on PHB plates

To test for the ability to utilize PHB as a sole carbon source, the isolates were grown on MSM-PHB plates in both aerobic and anaerobic conditions. They were incubated at 37°C for either 5 or 7 days and inspected for cell growth and a zone of clearing around the colonies. Five different agar media were tested, where the only difference was the nitrogen source.

SRB1LM and SRB3LM grew in aerobic conditions, while SRB7LM grew only when oxyrase was added to the minimal salt layer. Under those conditions all three isolates grew on all five nitrogen sources. Figures 11-13 depict images of the plates taken both with a regular camera and with higher resolution using a Bio-Rad gel imager. Only one plate for each isolate is shown here, the others can be found in the Appendix (from Figure S23 to Figure S28).

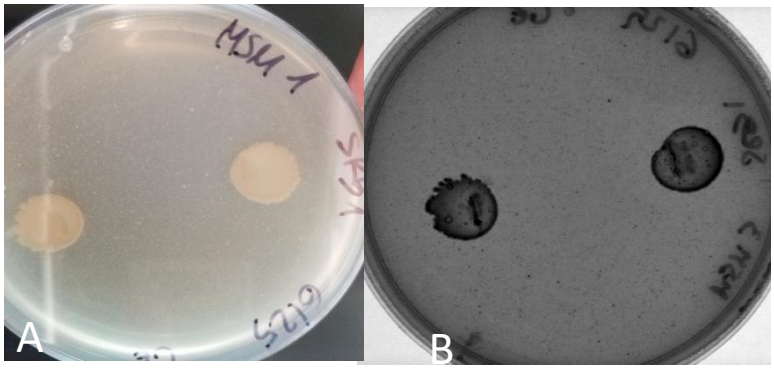

Figure 9: MSM-PHB agar plates, with 0.1% of PHB present as only carbon source; SRB1LM was inoculated (punctured into the plate which has a lower layer of MSM and a top layer of PHB solution 0.1%) and the plate incubated for 5-7 days at 37°C. (A) picture taken with a camera of the plate where two colonies can be seen. (B) picture of the same plate taken with a Bio-Rad gel imager.

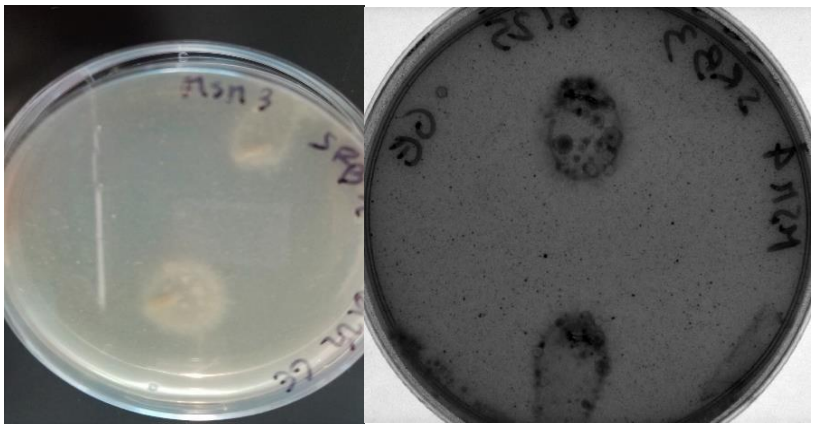

Figure 10: MSM-PHB agar plates, with 0.1% of PHB present as only carbon source; SRB3LM was inoculated (punctured into the plate which has a lower layer of MSM and a top layer of PHB solution 0.1%) and the plate incubated for 5-7 days at 37°C. (A) picture taken with a camera of the plate where two colonies can be seen. (B) picture of the same plate taken with a Bio-Rad gel imager.

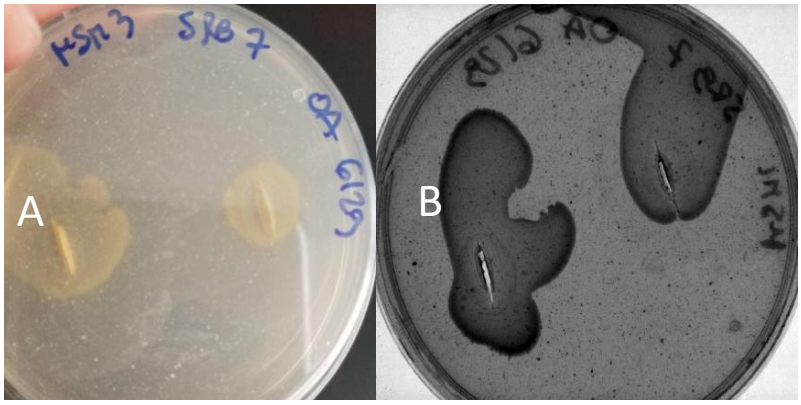

Figure 11: MSM-PHB agar plates, with 0.1% of PHB present as only carbon source; SRB7LM was inoculated (punctured into the plate which has a lower layer of MSM+oxyrase and a top layer of PHB solution 0.1%) and the plate incubated for 5-7 days at 37°C. (A) picture taken with a camera of the plate where two colonies can be seen. (B) picture of the same plate taken with a Bio-Rad gel imager.

Genome assembly

Three isolates (SRB1LM, SRB3LM, and SRB7LM) were selected for genome sequencing and their main features after the sequencing are shown in Table 4.

Table 4: Features of the DNA extracted from each isolate and their raw characteristics after sequencing.

Isolate	Final library DNA concentration (ng/µL)	Average library size (bp)	No. reads
SRB1LM	10.70	679	5,905,778
SRB3LM	8.24	644	5,431,640
SRB7LM	4.54	625	7,748,150

Genomes were assembled with three different programs: SPAdes, Velvet and MaSuRCA. Assembly metrics for all three assemblies for each isolate were compared using QUAST to select the best assembly for further analysis (Table 5). In the Appendix, a full report of assembly metrics can be found (from Figure S2 to Figure S4). For all three isolates Velvet produced the most contiguous assembly and was selected for further analysis, and a more detailed comparison of these assemblies for each isolate are shown in Table 6.

Table 5: Comparison between the assemblies obtained using Velvet, MaSuRCA and SPAdes.

SRB1_LM			
	Velvet	MaSuRCA	Spades
Number of contigs	43	105	133
Total length (bp)	5,950,746	5,887,191	5,873,426
N50 (bp)	745,621	206,967	192,084
GC (%)	35.18	35.18	35.13
SRB3_LM			
	Velvet	MaSuRCA	Spades
Number of contigs	123	155	230
Total length (bp)	6,545,436	5,745,734	5,901,766
N50 (bp)	478,895	154,758	157,736
GC (%)	35.13	35.23	35.15
SRB7_LM			
	Velvet	MaSuRCA	Spades
Number of contigs	10	21	86
Total length (bp)	2,890,966	2,832,629	2,889,993
N50 (bp)	2,758,154	469,934	1,926,999
GC (%)	48.04	47.93	47.83

Table 6: More detailed summary of the optimal genome assembly and annotation using QUAST for each of the three isolates.

Isolate	Genome size (bp)	Contigs	G+C content (%)	N50 (kbp)	Genes	RNAs
SRB1LM	5,950,746	43	35.18	745,621	6,263	145
SRB3LM	6,545,436	123	35.13	478,895	7,073	158
SRB7LM	2,890,966	10	48.04	2,758,154	2,970	91

Genome analysis

Once the genomes were assembled, a whole-genome Average Nucleotide Identity (ANI) comparison was performed, which allowed us to compare our assemblies with known genome assemblies. In Table 7, the top five average nucleotide identity (ANI) values between each isolate and all organisms in GenBank are demonstrated. For SRB1LM, all five ANI in the table belong to different strains of *Bacillus cereus.* Strains BcFL2013, G9241 and 03BB87 were isolated from patients, while FM1 was isolated from dried foods (Carter et al., 2018).

The five highest values for SRB3LM are all from members of *Bacillus*; three *B. cereus* and two *B. thuringensis.* Not much information is available about these strains, but *Bacillus cereus* M13(2017) was isolated from the soils of Kanas lake in Xinjiang Uigur, an autonomous Region of northwest China.

Isolate SRB7LM has an ANI value higher than 95% with two separate strains belonging to the *Exiguobacterium* genus. Members of this genus have been isolated from a multitude of environments, ranging from glaciers to hot springs (Kasana and Pandey, 2018; Vishnivetskaya et al., 2009). As of today, there are 17 species in the genus *Exiguobacterium* and it is a pretty versatile genus with lots of potential in industry, for example in bioremediation processes (Kasana and Pandey, 2018).

Table 7: The top five highest average nucleotide identity (ANI) values between each of the three isolates and all organisms in GenBank. Italicized values indicate an ANI over the intra-species threshold.

SRB1LM	
***Bacillus cereus* BcFL2013**	*97.97*
***Bacillus cereus* FM1**	*97.92*

***Bacillus cereus* G9241**	*97.86*
***Bacillus cereus* 03BB87**	*97.82*
***Bacillus cereus* ATCC 4342**	*97.41*
SRB3LM	
***Bacillus cereus* VD014**	*98.86*
***Bacillus cereus* M13(2017)**	*98.78*
***Bacillus thuringiensis* BGSC 4BD1**	*98.74*
***Bacillus thuringiensis* 78-2**	*98.73*
***Bacillus cereus* VD156**	*98.67*
SRB7LM	
***Exiguobacterium sp.* NG55**	*95.40*
***Exiguobacterium sp.* AT1b**	*95.29*
***Exiguobacterium marinum* DSM 16308**	88.41
***Exiguobacterium aurantiacum* DSM 6208**	81.31
***Exiguobacterium chiriqhucha* GIC31**	81.20

In Table S1 in the Appendix, a summary of the lineage of each isolate is demonstrated.

The identities of three isolates were explored further by building genome-scale phylogenetic trees. Based on their ANI comparisons, SRB1LM and SRB3LM were included in one tree containing all representative members in *Bacillus* within the PATRIC database (Figure 12). A second tree was built for SRB7LM that included every *Exiguobacterium* genome in the PATRIC database (Figure 13). SRB1LM's closest neighbor is a strain of *B. anthracis*, while the closest neighbor of SRB3LM is a strain of *B. thuringenis*. This result confirms those of fastANI, as both *B. thuringenis* and *anthracis* are genetically very close to *B. cereus* and they could actually be considered one species (Helgason et al., 2000; Radnedge et al., 2003). SRB7LM's closest neighbors are strains of *Exiguobacterium*, two of them (*E. profundum* and *E. marinum*) were also isolated from the marine environment (Crapart et al., 2007; Kim, 2005).

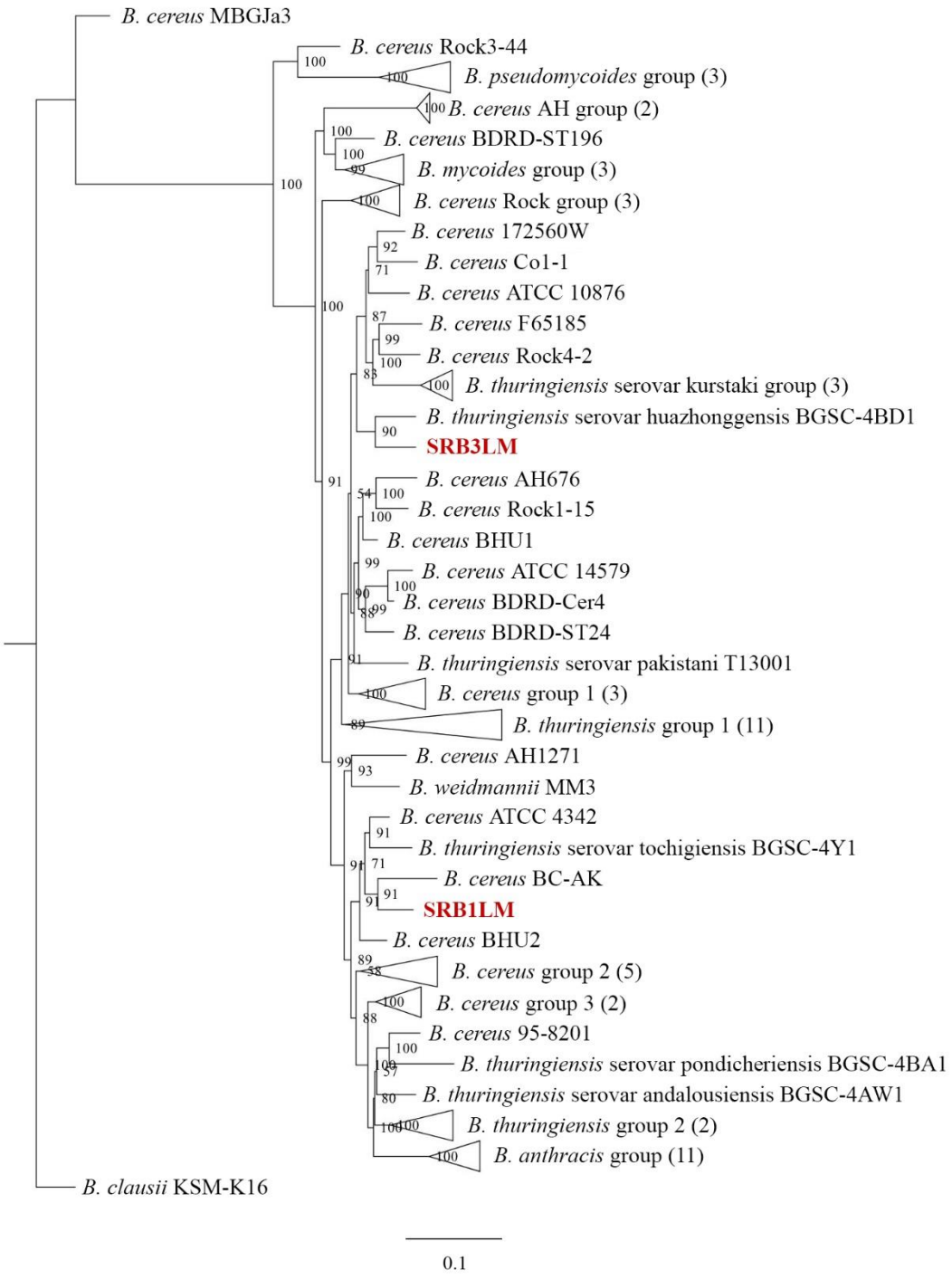

Figure 12: Maximum-likelihood phylogenetic tree based on PATRIC's comprehensive genome analysis service. 98 genomes within *Bacillus* in the PATRIC database were included in the tree. The position of isolates SRB1LM and SRB3LM is highlighted in yellow.Node labels show the bootstrap support values, and values of 100% are not shown. Branch lengths represent the average number of substitutions per site. The tree was rooted to a more distantly related *Bacillaceae* (*Halobacillus sp.* BBL2006). When strains from the same species were present on one branch, they were all

combined in one single branch and labeled as a single group; in the parenthesis it is indicated the number of strains that are present in that group.

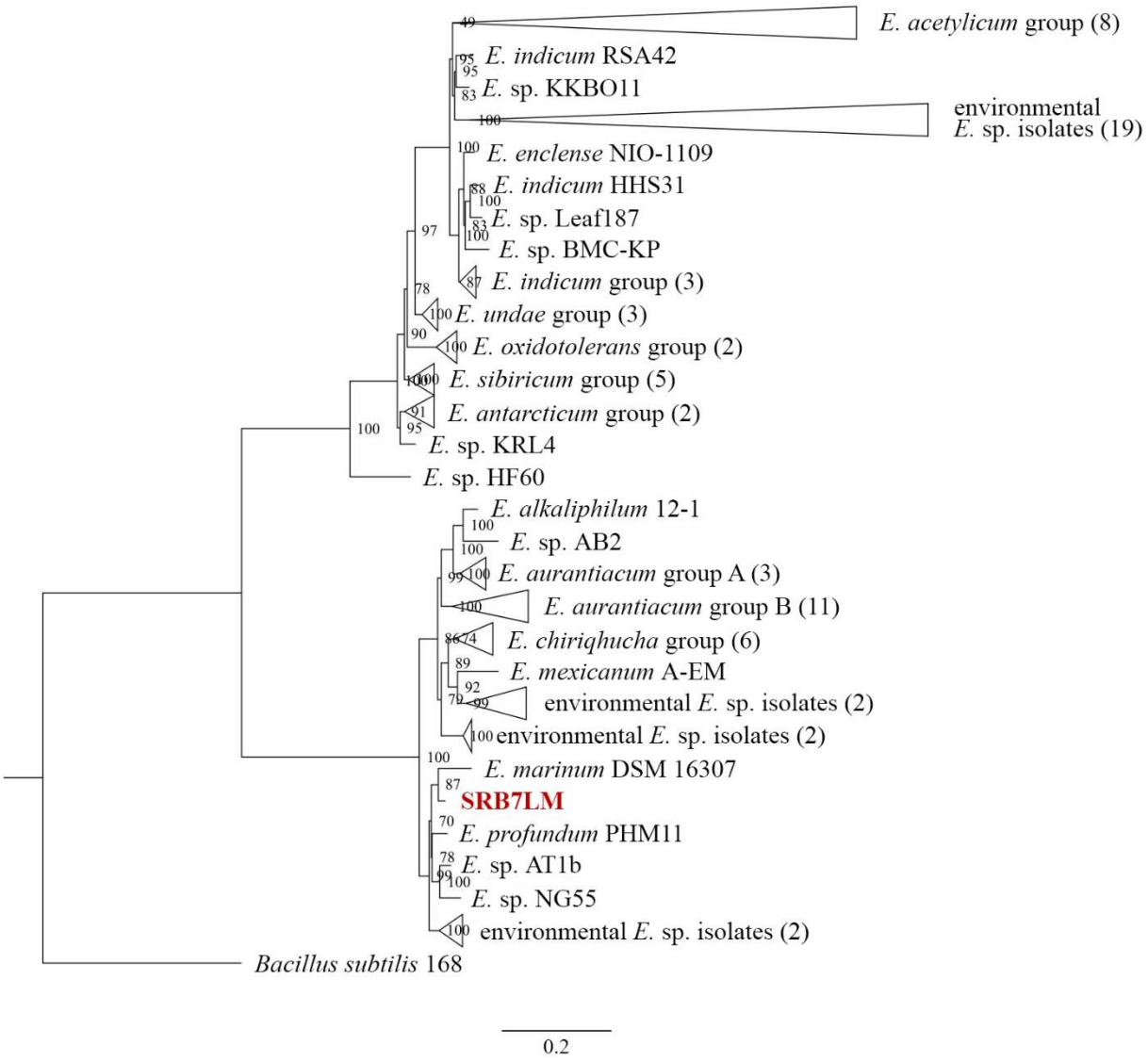

Figure 13: Maximum-likelihood phylogenetic tree based on PATRIC's comprehensive genome analysis service. 75 genomes within *Exiguobacterium* in the PATRIC database were included in the tree. The position of isolate SRB7LM is highlighted in yellow.Node labels show the bootstrap support values, and values of 100% are not shown. Branch lengths represent the average number of substitutions per site. The tree was rooted to a more distantly related *Bacillaceae* (*Bacillus cereus* G9241). When strains from the same species were present on one branch, they were all combined in one single branch and labeled as a single group; in the parenthesis it is indicated the number of strains that are present in that group.

Genomic potential of PHA degradation and sulphate reduction

To characterize each isolate's potential for both sulfate reduction and PHA degradation, a search for genes involved in sulphate reduction and also PHB degradation was conducted. SRB1LM and SRB3LM contained the same genes involved in PHA degradation pathways (phaZ and PHA depolymerase aromatic) and in the sulphate reduction pathways. They both contained genes involved in both the dissimilatory reduction of sulphate (dsrA and dsrB) and assimilatory reduction of sulphate (sopT, sulphate reductase subunit B and C). SRB7LM differed from SRB1LM and SRB3LM. It contained a PHA depolymerase aromatic gene and a sulphate reductase subunit B gene. Table 8 reports the number of positive hits for each gene within each isolate.

Table 8: Number of found matches between genes of the isolates and known genes responsible for the degradation of PHA and known genes involved in the assimilatory and dissimilatory sulphate reduction pathways. E-value of 10^{-5} is the threshold that divides a positive match (lower E-value than 10^{-5}) and a random hit (higher E-value than 10^{-5}).

	SRB1LM # of hits	**SRB3LM # of hits**	**SRB7LM # of hits**
PHB depolymerase (intracellular). phaZ	1	1	No hits
PHA depolymerase aromatic	13	9	3
Esterase PHB	No hits	No hits	No hits
Sulfite reductase (dissimilatory type, alpha subunit). dsrA	2	2	No hits
Sulfite reductase (dissimilatory type, beta subunit). dsrB	1	1	No hits
Sulfate adenylyltransferase. sopT	1	1	No hits
Sulfate reductase (subunit B)	1	1	1
Sulfate reductase (subunit C)	4	4	No hits

Discussion

This study characterized three individual members of microbial communities forming biofilms on PHA pellets at the sediment-water interface. Through selective isolation and whole-genome sequencing, this study addressed whether SRM capable of degrading PHA were part of the biofilm community. In the predicted scenario of increased bioplastic loading, this study provided important information about the effect increased PHA loading would have on marine microorganisms and sulfur cycling in coastal marine sediments.

Through the implementation of two different steps using two specific liquid media, the isolation procedure produced nine total isolates capable of growing in SRB and PHB-MSM media. Of these, three isolates with differing morphologies were selected for whole-genome sequencing. The genome size for SRB7LM was considerable smaller (2.8 Mbp) versus both SRB1LM and SRB3LM (6.0 Mbp), signifying they likely belong to different species as it is well established that different species vary in size due to differing evolutionary histories (Bobay and Ochman, 2017). Additionally, starkly different GC content between SRB7LM (48%) and SRB1LM/SRB3LM (35%) suggested that SRB7LM differs from the other two isolates. Interestingly, GC content is one of the main compositional diversity of bacteria (Brocchieri, 2014). While, the difference in GC content between SRB7LM and the other two isolates is considerable, they are all part of the same phylum (Firmicutes), which typically have a low GC content (Lightfield et al., 2011)).

To determine their phylogenetic relatedness, all three isolates were compared to known organisms with fastANI and placed into a maximum-likelihood phylogenetic tree. SRB1LM and SRB3LM were classified as two strains of *Bacillus*, with their closest neighbours being strains of *B. thuringensis* and *B. cereus*, respectively. The genus *Bacillus* is large and very diverse (Cihan et al., 2012; Yakoubou and Côté 2010). Members of *Bacillus* are commonly found in both water and sediment (George et al., 2011), thus the presence of strains of this genus at the sediment-water interface of the Laguna Madre was not surprising. SRB7LM was placed in the genus *Exiguobacterium*, which is similar to *Bacillus* and is part of the phylum Firmicutes. The ANI results showed that SRB7LM belongs to the same species of a strain of *Exiguobacterium* named *Exiguobacterium sp.* NG55 since the ANI value is higher than 95, thus indicating that the two strains are intraspecies (Jain et al., 2018). This

strain was isolated from a hot spring in Yellowstone National Park (Vishnivetskaya et al., 2009). In addition, the next two closest neighbors of SRB7LM were two species of *Exiguobacterium* isolated from the marine environment (*E. marinum* and *E. profundum*) (Crapart et al., 2007; Kim, 2005). Interestingly, this genus has been isolated from a large variety of environments, ranging from hot springs to glaciers (Kasana and Pandey, 2018). Bacteria belonging to this genus also have a genome size similar to SRB7LM's genome (around 3 million bp) and a GC content close to 50% (Vishnivetskaya et al., 2009). As said before, strains from this genus were isolated from extreme environments like hot springs, meaning that they are thermophilic bacteria; more studies would need to be done, but SRB7LM may also be a thermophilic bacterium.

In order to determine each isolate's potential to degrade PHA and reduce sulphate, draft genomes were searched for PHA depolymerases and sulfate reduction genes. While all three isolates did contain depolymerase gene sequences, they were more prevalent in SRB1LM and SRB3LM. As a matter of fact, the two *Bacillus* strains have the gene for phaZ, which is a PHA depolymerase of the BCL-PHA depolymerase class; depolymerases in this class are able to degrade PHB and its co-polyesters (Roohi et al., 2018). Instead, all three isolates have genes for a PHA depolymerase aromatic, which instead belongs to the second class of PHA depolymerases, called MCL-PHA. These type of depolymerases are able to degrade longer aliphatic PHAs and also aromatic PHAs (Roohi et al., 2018); SBRB7LM thus has the potential of degrading PHA, however in this study no aromatic PHAs were used. Additionally, the two isolated *Bacillus* (SRB1LM and SRB3LM) strains possessed genes for dissimilatory sulphate reduction. In particular, they both contained gene sequences for *dsrA* and *dsrB*, which reduce sulphate to sulfide (Castro et al., 2000; Gibson, 1990). Interestingly, *Bacillus* are not known to use the dissimilatory pathway of sulphate reduction, but some of them do however have the ability to use nitrite as electron acceptor (Hoffmann et al., 1998). This result could place the two isolates in the Gram-positive spore forming SRBs group. SRB7LM did not have any sulphate reduction genes in its genome and nothing was found in the literature about any other species of the genus being able to use other electron acceptors.

Most species of *Bacillus* and *Exiguobacterium* are facultative anaerobes (Cihan et al., 2012; Vishnivetskaya et al., 2009), which was supported by the results of this study as all

three isolates were isolated in anaerobic conditions but were also able to grow in aerobic conditions. Moreover, their growth in a complex liquid medium demonstrated a higher OD_{600} under aerobic conditions. Importantly, this does not necessarily mean that they have a higher growth rate, but simply a higher yield in those conditions. Interestingly, under most of the conditions, the growth rates of the isolates were higher under anaerobic conditions, which was especially true for SRB7LM.

The most challenging part of this study was the *in vitro* demonstration that the isolates could degrade PHB in laboratory conditions, but results demonstrated that they can grow on agar plates where the only carbon source was PHB. It is well documented in the literature that a large number of *Bacillus* species are known PHA producers, and that the extraction of PHA from their cytoplasm is easier compared to other bacterial species (Mohapatra et al., 2017). In addition, *Bacillus* species were found amongst those able to degrade PHA in a previous study (Volova et al., 2017). Contrastingly, nothing in the literature supports that members of *Exiguobacterium* degrade or produce PHA. However, a species of *Exiguobacterium* was present in the gut of plastic-eating mealworms (Yang et al., 2015), suggesting that there might be species or strains of *Exiguobacterium* that are able to degrade complex polymers such as bioplastics. It needs to be noted that SRB7LM was able to grow on PHB plates only when oxyrase was added to the MSM layer of the plates; in the oxyrase preparation a small amount of other carbon sources is present, thus it could either mean that SRB7LM is using only that traces of C sources to grow or that it is using those traces and also PHB. For this specific reason, SRB7LM can be considered a potential PHA degraders, but it cannot be said with certainty that it actually is a PHA degrader.

In conclusion, this study isolated three bacteria from biofilms formed on PHA pellets at the sediment-water interface and demonstrated they have the genomic capability to both degrade PHA and play a role in sulphate reduction. Their ability to degrade PHA was also shown *in vitro*, with the isolates growing on media containing PHB as the sole carbon source. Interestingly, that the two isolates belonging to the *Bacillus* genus contained genes involved in the dissimilatory reduction of sulphate is something that had not been demonstrated in the literature with species of *Bacillus*. These bacteria could then also be used industrially because of their potential to degrade PHA and their ability to grow also when sulphate concentration is high. As a matter of fact, not all PHA degraders are SRBs and

also not all SRBs are PHA degraders; the fact that these strains have both these features might pose as an advantage because the predicted increase in PHA production may result in higher PHA deposition rates in coastal sediments, which coupled with the already high concentration of sulphate (Rabus et al., 2015) could result in growth conditions favoring these types of bacteria.

References

Aeschelmann, F. and Carus, M., 2015. Biobased building blocks and polymers in the world: capacities, production, and applications–status quo and trends towards 2020. Industrial Biotechnology 11 (3), 154. https://doi.org/10.1089/ind.2015.28999.fae.

Andrady, A.L., 2011. Microplastics in the marine environment. Marine Pollution Bulletin 62: 1596-1605. https://doi.org/10.1016/j.marpolbul.2011.05.030

Andrews S. (2010). FastQC: a quality control tool for high throughput sequence data. Available online at: http://www.bioinformatics.babraham.ac.uk/projects/fastqc.

Bankevich, A., Nurk, S., Antipov, D., Gurevich, A.A., Dvorkin, M., Kulikov, A.S., Lesin, V.M., Nikolenko, S.I., Pham, S., Prjibelski, A.D., Pyshkin, A.V., Sirotkin, A.V., Vyahhi, N., Tesler, G., Alekseyev, M.A., and Pevzner, P.A., 2012. SPAdes: A new genome assembly algorithm and its applications to single-cell sequencing. Journal of Computational Biology 19(5), 455-477. doi:10.1089/cmb.2012.0021.

Barnes, D.K., Galgani, F., Thompson, R.C., Barlaz, M., 2009. Accumulation and fragmentation of plastic debris in global environments. Philosophical Transactions of the Royal Society London B: Biological Sciences 364, 1985-1998. https://doi.org/10.1098/rstb.2008.0205

Brettin, T., Davis, J.J., Disz, T., Edwards, R.A., Gerdes, S., Olsen, G.J., Olson, R., Overbeek, R., Parrello, B., Pusch, G.D., Shukla, M., Thomason, J.A., Stevens, R., Vonstein, V., Wattam, A.R., Xia, F., 2015. RASTtk: A modular and extensible implementation of the RAST algorithm for building custom annotation pipelines and annotating batches of genomes. Scientific Reports 5. https://doi.org/10.1038/srep08365

Carter, L., Chase, H.R., Gieseker, C.M., Hasbrouck, N.R., Stine, C.B., Khan, A., Ewing-Peeples, L.J., Tall, B.D., Gopinath, G.R., 2018. Analysis of enterotoxigenic *Bacillus cereus* strains from dried foods using whole genome sequencing, multi-locus sequence analysis and toxin gene prevalence and distribution using endpoint PCR analysis. International Journal of Food Microbiology 284, 31–39. https://doi.org/10.1016/j.ijfoodmicro.2018.06.016

Castro, H.F., Williams, N.H., Ogram, A., (2000). Phylogeny of sulphate reducing bacteria. FEMS Microbiology Ecology 31: 1–9. doi: 10.1111/j.1574-6941.2000.tb00665.x

Chatterjee, S., Sharma, S., 2019. Microplastics in our oceans and marine health. Field Actions Science Reports 19, 54-61. http://journals.openedition.org/factsreports/5257

Çetin, D., 2009. Anaerobic Biodegradation of Poly-3-Hydroxybutyrate (PHB) by Sulfate Reducing Bacterium *Desulfotomaculum* sp. Soil and Sediment Contamination: An International Journal 18, 345–353. https://doi.org/10.1080/15320380902772653

Cihan, A.C., Tekin, N., Ozcan, B., Cokmus, C., 2012. The genetic diversity of genus *Bacillus* and the related genera revealed by 16S rRNA gene sequences and ardra analyses isolated from geothermal regions of turkey. Brazilian Journal of Microbiology 43, 309–324. https://doi.org/10.1590/S1517-83822012000100037.

Crapart, S., Fardeau, M.-L., Cayol, J.-L., Thomas, P., Sery, C., Ollivier, B., Combet-Blanc, Y., 2007. *Exiguobacterium profundum* sp. nov., a moderately thermophilic, lactic acid-producing bacterium isolated from a deep-sea hydrothermal vent. International Journal of Systematic and Evolutionary Microbiology 57, 287–292. https://doi.org/10.1099/ijs.0.64639-0

Cruz Ramos, H., Hoffmann, T., Marino, M., Nedjari, H., Presecan-Siedel, E., Dreesen, O., Glaser, P., Jahn, D., 2000. Fermentative metabolism of *Bacillus subtilis*: physiology and regulation of gene expression. Journal of Bacteriology 182, 3072–3080. https://doi.org/10.1128/JB.182.11.3072-3080.2000

Edgar, R.C., 2004. MUSCLE: multiple sequence alignment with high accuracy and high throughput. Nucleic Acids Research 32, 1792–1797. https://doi.org/10.1093/nar/gkh340.

European bioplastics. 2019. What are bioplastics?. [ONLINE] Available at: https://www.european-bioplastics.org/bioplastics/. [Accessed 21 June 2019].

Finn, R.D., Clements, J., Eddy, S.R., 2011. HMMER web server: interactive sequence similarity searching. Nucleic Acids Research 39, W29–W37. https://doi.org/10.1093/nar/gkr367.

Flemming, H.-C., Wingender, J., Szewzyk, U., Steinberg, P., Rice, S.A., Kjelleberg, S., 2016. Biofilms: an emergent form of bacterial life. Nature Reviews Microbiology 14, 563. doi: 10.1038/nrmicro.2016.94.

George, M., Cyriac, N., Nair, A., 2011. Diversity of *Bacillus* and *Actinomycetes* in the water and sediment samples from Kumarakom region of Vembanadu lake. Indian Journal of Marine

Sciences, 40, 8. https://pdfs.semanticscholar.org/4a7e/2c3550ca441f8eca9cabea9cedc9f585b204.pdf

Geyer, R., Jambeck, J.R., Law, K.L., 2017. Production, use, and fate of all plastics ever made. Science Advances 3, e1700782.Doi: 10.1126/sciadv.1700782

Grein, F., Ramos, A.R., Venceslau, S.S., Pereira, I.A.C., 2013. Unifying concepts in anaerobic respiration: Insights from dissimilatory sulphur metabolism. Biochimica et Biophysica Acta (BBA) - Bioenergetics 1827, 145–160. https://doi.org/10.1016/j.bbabio.2012.09.001.

Gurevich, A., Saveliev, V., Vyahhi, N., Tesler, G., 2013. QUAST: quality assessment tool for genome assemblies. Bioinformatics 29, 1072–1075. https://doi.org/10.1093/bioinformatics/btt086

Helgason, E., Okstad, O.A., Caugant, D.A., Johansen, H.A., Fouet, A., Mock, M., Hegna, I., Kolsto, A.-B., 2000. *Bacillus anthracis*, *Bacillus cereus*, and *Bacillus thuringiensis*---one species on the basis of genetic evidence. Applied and Environmental Microbiology 66, 2627–2630. https://doi.org/10.1128/AEM.66.6.2627-2630.2000.

Hoffmann, T., Frankenberg, N., Marino, M., Jahn, D., 1998. Ammonification in *Bacillus subtilis* utilizing dissimilatory nitrite reductase is dependent on *res*DE. Journal of Bacteriology 180, 186–189. https://jb.asm.org/content/180/1/186

Hoseinabadi, A., Rasooli, I., Taran, M., 2015. Isolation and identification of poly β-hydroxybutyrate over-producing bacteria and optimization of production medium. Jundishapur Journal of Microbiology 8. https://doi.org/10.5812/jjm.16965v2.

Hyatt, D., Chen, G.-L., LoCascio, P.F., Land, M.L., Larimer, F.W., Hauser, L.J., 2010. Prodigal: prokaryotic gene recognition and translation initiation site identification. BMC Bioinformatics 11. https://doi.org/10.1186/1471-2105-11-119.

Jain, C., Rodriguez-R, L.M., Phillippy, A.M., Konstantinidis, K.T., Aluru, S., 2018. High throughput ANI analysis of 90K prokaryotic genomes reveals clear species boundaries. Nature Communications 9. https://doi.org/10.1038/s41467-018-07641-9.

Jonkers, H., Koh, IO., Behrend, P. Muyzer, G., de Beer, D., 2005. Aerobic organic carbon mineralization by sulfate-reducing bacteria in the oxygen-saturated photic zone of a

hypersaline microbial mat. Microbial Ecology 49: 291. https://doi.org/10.1007/s00248-004-0260-y.

Jørgensen, B.B., 1982. Mineralization of organic matter in the sea-bed — the role of sulphate reduction, Nature 390 364–370. https://dx.doi.org/10.3389%2Ffmicb.2013.00209

Kasana, R.C., Pandey, C.B., 2018. *Exiguobacterium* : an overview of a versatile genus with potential in industry and agriculture. Critical Reviews in Biotechnology 38, 141–156. https://doi.org/10.1080/07388551.2017.1312273.

Keskin, G., Kızıl, G., Bechelany, M., Pochat-Bohatier, C., Öner, M., 2017. Potential of polyhydroxyalkanoate (PHA) polymers family as substitutes of petroleum based polymers for packaging applications and solutions brought by their composites to form barrier materials. Pure and Applied Chemistry 89, 1841–1848. https://doi.org/10.1515/pac-2017-0401

Kim, I.-G., 2005. *Exiguobacterium aestuarii* sp. nov. and *Exiguobacterium marinum* sp. nov., isolated from a tidal flat of the Yellow Sea in Korea. International Journal of Systematic and Evolutionary Microbiology 55, 885–889. https://doi.org/10.1099/ijs.0.63308-0.

Lavers, J., Hutton, I., Bond, A., 2018. Ingestion of marine debris by Wedge-tailed Shearwaters (*Ardenna pacifica*) on Lord Howe Island, Australia during 2005-2018. Marine pollution bulletin 133, 616–621. doi: 10.1016/j.marpolbul.2018.06.023

Li, L., 2003. OrthoMCL: Identification of ortholog groups for eukaryotic genomes. Genome Research 13, 2178–2189. https://doi.org/10.1101/gr.1224503.

Lightfield, J., Fram, N.R., Ely, B., 2011. Across bacterial phyla, distantly-related genomes with similar genomic GC content have similar patterns of amino acid usage. PLoS ONE 6, e17677. https://doi.org/10.1371/journal.pone.0017677

Mabrouk, M.M., Sabry, S.A., 2001. Degradation of poly (3-hydroxybutyrate) and its copolymer poly (3-hydroxybutyrate-co-3-hydroxyvalerate) by a marine *Streptomyces* sp. SNG9. Microbiological Research 156, 323–335. https://doi.org/10.1078/0944-5013-00115.

Magoč, T., and S. L. Salzberg. 2011. FLASH: fast length adjustment of short reads to improve genome assemblies. Bioinformatics 27: 2957– 2963. doi: 10.1093/bioinformatics/btr507.

Martin, M., 2011. Cutadapt removes adapter sequences from high-throughput sequencing reads. EMBnet.journal, [S.l.], v. 17, n. 1; 10-12. https://doi.org/10.14806/ej.17.1.200

Mohapatra, S., Maity, S., Dash, H.R., Das, S., Pattnaik, S., Rath, C.C., Samantaray, D., 2017. *Bacillus* and biopolymer: prospects and challenges. Biochemistry and Biophysics Reports 12, 206–213. https://doi.org/10.1016/j.bbrep.2017.10.001.

Nehra, K., Jaglan, A., Shaheen, A., Yadav, J., Lathwal, P., 2015. Production of Poly-β-Hydroxybutyrate (PHB) by bacteria isolated from rhizospheric soils. International Journal Microbial Resource Technology, Vol.2, No. 3. https://pdfs.semanticscholar.org/cd8b/8d8dd127e602b5e80097129361ccb8b31272.pdf

Okeke, B.C., 2008. Bioremoval of hexavalent chromium from water by a salt tolerant bacterium, *Exiguobacterium* sp. GS1. Journal of Industrial Microbiology Biotechnology, 35: 1571-1579. https://doi.org/10.1007/s10295-008-0399-5.

Ondov, B.D., Treangen, T.J., Melsted, P., Mallonee, A.B., Bergman, N.H., Koren, S., Phillippy, A.M., 2016. Mash: fast genome and metagenome distance estimation using MinHash. Genome Biology 17, 132. https://doi.org/10.1186/s13059-016-0997-x.

Pinnell, L.J., Turner, J.W., 2019. Shotgun metagenomics reveals the benthic microbial community response to plastic and bioplastic in a coastal marine environment. Frontiers in Microbiology 10. https://doi.org/10.3389/fmicb.2019.01252

Prados, E., Maicas, S., 2016. Bacterial Production of Hydroxyalkanoates (PHA). Universal Journal of Microbiology Research 4(1): 23-30. Doi: 10.13189/ujmr.2016.040104

Rabus, R., Venceslau, S.S., Wöhlbrand, L., Voordouw, G., Wall, J.D., Pereira, I.A.C., 2015. A post-genomic view of the ecophysiology, catabolism and biotechnological relevance of sulphate-reducing prokaryotes. Advances in Microbial Physiology. Elsevier, pp. 55–321. https://doi.org/10.1016/bs.ampbs.2015.05.002.

Radnedge, L., Agron, P.G., Hill, K.K., Jackson, P.J., Ticknor, L.O., Keim, P., Andersen, G.L., 2003. Genome differences that distinguish *Bacillus anthracis* from *Bacillus cereus* and *Bacillus*

thuringiensis. Applied and Environmental Microbiology 69, 2755–2764. https://doi.org/10.1128/AEM.69.5.2755-2764.2003.

Reddy, S., Thirumala, M., Mahmood, S., 2007. Biodegradation of polyhydroxyalkanoates. The Internet Journal of Microbiology, Volume 4 Number 2. https://pdfs.semanticscholar.org/3494/174107c178a4cb5baa81f90b3678df2ab9cb.pdf

Roohi, Zaheer, M.R., Kuddus, M., 2018. PHB (poly-β-hydroxybutyrate) and its enzymatic degradation. Polymers for Advanced Technologies 29, 30–40. https://doi.org/10.1002/pat.4126

Setälä, O. , Fleming-Lehtinen, V. , Lehtiniemi, M., 2014 Ingestion and transfer of microplastics in the planktonic food web. Environmental Pollution 185, 77-83. doi: 10.1016/j.envpol.2013.10.013

Stamatakis, A., 2014. RAxML version 8: a tool for phylogenetic analysis and post-analysis of large phylogenies. Bioinformatics 30, 1312–1313. https://doi.org/10.1093/bioinformatics/btu033

Taguchi, Y., Sugishima, M., Fukuyama, K., 2004. Crystal structure of a novel zinc-binding ATP sulfurylase from *Thermus thermophilus* HB8. Biochemistry 43, 4111–4118. https://doi.org/10.1021/bi036052t.

Talavera, G., Castresana, J., 2007. Improvement of phylogenies after removing divergent and ambiguously aligned blocks from protein sequence alignments. Systematic Biology 56, 564–577. https://doi.org/10.1080/10635150701472164.

Tan, G.-Y., Chen, C.-L., Li, L., Ge, L., Wang, L., Razaad, I., Li, Y., Zhao, L., Mo, Y., Wang, J.-Y., 2014. Start a research on biopolymer polyhydroxyalkanoate (PHA): A Review. Polymers 6, 706–754. https://doi.org/10.3390/polym6030706.

Tan, L., Qu, Y., Zhou, J., Li, A., Gou, M., 2009. Identification and characteristics of a novel salt-tolerant *Exiguobacterium* sp. for azo dyes decolorization. Applied Biochemistry and Biotechnology 159: 728. https://doi.org/10.1007/s12010-009-8546-7.

Thammasittirong, A., Saechow, S., Thammasittirong, S.N.-R., 2017. Efficient polyhydroxybutyrate production from *Bacillus thuringiensis* using sugarcane juice substrate. Turkish Journal of Biology 41, 992–1002. https://doi.org/10.3906/biy-1704-13.

Ullrich, T.C., 2001. Crystal structure of ATP sulfurylase from *Saccharomyces cerevisiae*, a key enzyme in sulphate activation. The EMBO Journal 20, 316–329. https://doi.org/10.1093/emboj/20.3.316.

Vigneswari, S., Lee, T.S., Bhubalan, K., Amirul, A.A., 2015. Extracellular polyhydroxyalkanoate depolymerase by *Acidovorax* sp. DP5. Enzyme Research 2015, 1–8. https://doi.org/10.1155/2015/212159.

Vijayalaxmi, S., Anu Appaiah, K.A., Jayalakshmi, S.K., Mulimani, V. H. , Sreeramulu, K., 2013. Production of bioethanol from fermented sugars of sugarcane bagasse produced by lignocellulolytic enzymes of *Exiguobacterium* sp. VSG-1. Applied Biochemistry Biotechnology, 171: 246-260. https://doi.org/10.1007/s12010-013-0366-0

Vishnivetskaya, T.A., Chauhan, A., Layton, A.C., Pfiffner, S.M., Huntemann, M., Copeland, A., Chen, A., Kyrpides, N.C., Markowitz, V.M., Palaniappan, K., Ivanova, N., Mikhailova, N., Ovchinnikova, G., Andersen, E.W., Pati, A., Stamatis, D., Reddy, T.B.K., Shapiro, N., Nordberg, H.P., Cantor, M.N., Hua, X.S., Woyke, T., 2014. Draft genome sequences of 10 strains of the genus *Exiguobacterium*. Genome Announcements. https://doi.org/10.1128/genomeA.01058-14.

Volova, T.G., Prudnikova, S.V., Vinogradova, O.N., Syrvacheva, D.A., Shishatskaya, E.I., 2017. Microbial degradation of polyhydroxyalkanoates with different chemical compositions and their biodegradability. Microbial Ecology 73, 353–367. https://doi.org/10.1007/s00248-016-0852-3.

Wasmund, K., Mußmann, M., Loy, A., 2017. The life sulfuric: microbial ecology of sulfur cycling in marine sediments: Microbial sulfur cycling in marine sediments. Environmental Microbiology Reports 9, 323–344. https://doi.org/10.1111/1758-2229.12538.

Wattam, A.R., Davis, J.J., Assaf, R., Boisvert, S., Brettin, T., Bun, C., Conrad, N., Dietrich, E.M., Disz, T., Gabbard, J.L., Gerdes, S., Henry, C.S., Kenyon, R.W., Machi, D., Mao, C., Nordberg, E.K., Olsen, G.J., Murphy-Olson, D.E., Olson, R., Overbeek, R., Parrello, B., Pusch, G.D., Shukla, M.,

Vonstein, V., Warren, A., Xia, F., Yoo, H., Stevens, R.L., 2017. Improvements to PATRIC, the all-bacterial bioinformatics database and analysis resource center. Nucleic Acids Research 45, D535–D542. https://doi.org/10.1093/nar/gkw1017.

Yakoubou, S., Côté, J.-C., 2010. Assessment of a short phylogenetic marker based on comparisons of 3' end 16S rDNA and 5' end 16S-23S ITS nucleotide sequences of the Bacillus cereus group. Natural Science 02, 1113–1118. https://doi.org/10.4236/ns.2010.210138.

Yang, Y., Yang, J., Wu, W.-M., Zhao, J., Song, Y., Gao, L., Yang, R., Jiang, L., 2015. Biodegradation and mineralization of polystyrene by plastic-eating mealworms: part 1. Chemical and physical characterization and isotopic tests. Environmental Science & Technology 49, 12080–12086. https://doi.org/10.1021/acs.est.5b02661

Zerbino, D.R., Birney, E., 2008. Velvet: Algorithms for de novo short read assembly using de Bruijn graphs. Genome Research 18, 821–829. https://doi.org/10.1101/gr.074492.107

Zimin, A.V., Marçais, G., Puiu, D., 2013. The MaSuRCA genome assembler. Bioinformatics, 29:2669–77. Doi: 10.1093/bioinformatics/btt476

Appendix

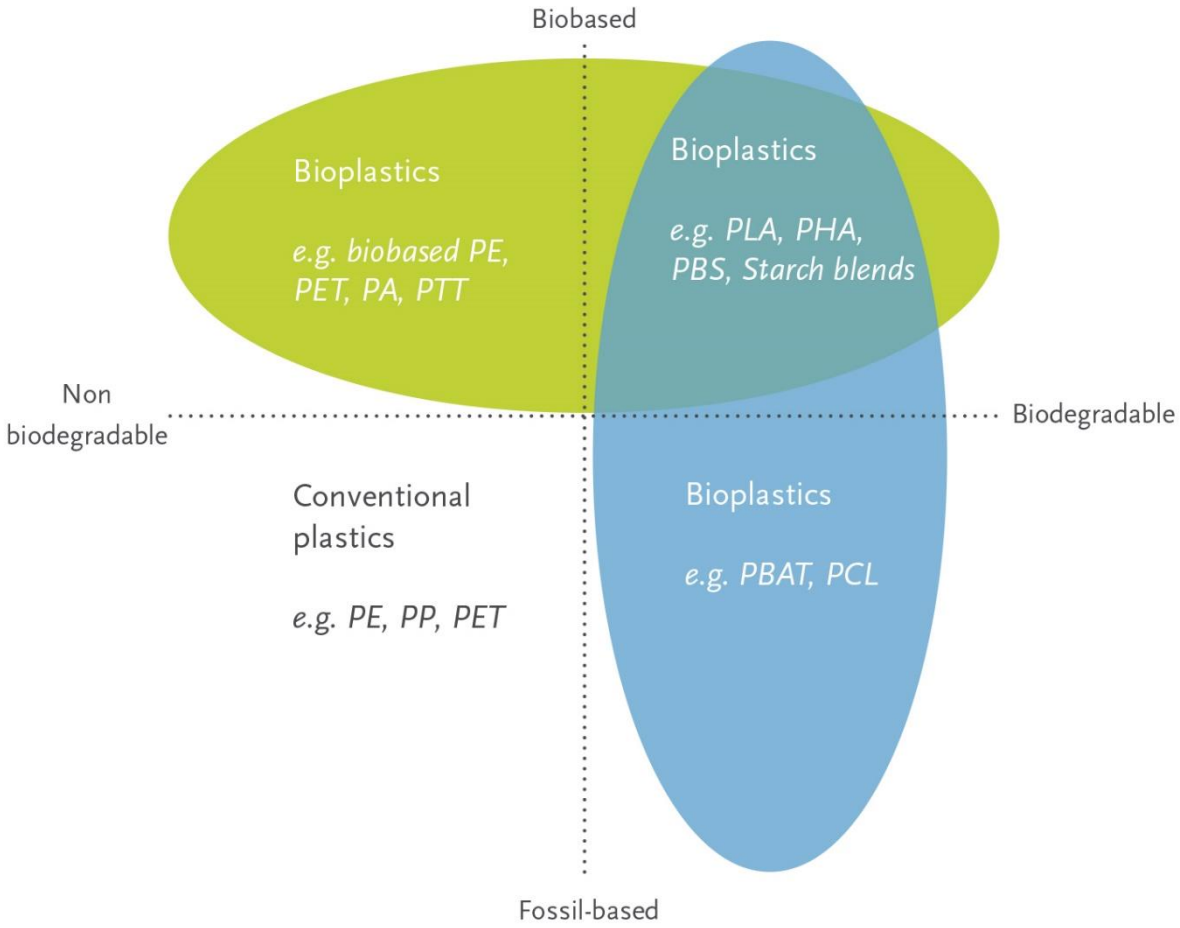

Figure S1: Difference between conventional plastics and the so called bioplastics. (European bioplastic)

Quast results

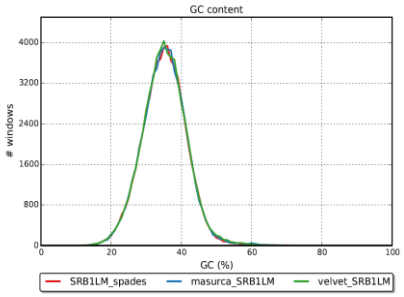

(A)

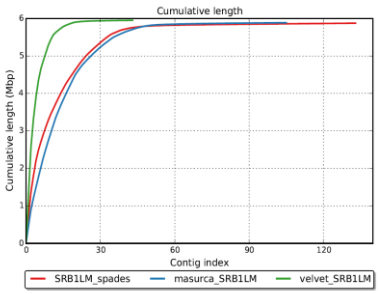

(B

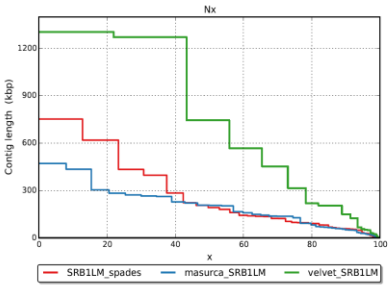

(C

Report

	SRB1LM_spades	masurca_SRB1LM	velvet_SRB1LM
# contigs (>= 0 bp)	890	125	43
# contigs (>= 1000 bp)	66	72	34
# contigs (>= 5000 bp)	47	51	22
# contigs (>= 10000 bp)	42	48	20
# contigs (>= 25000 bp)	38	40	17
# contigs (>= 50000 bp)	32	33	14
Total length (>= 0 bp)	6068508	5894740	5950746
Total length (>= 1000 bp)	5828659	5864296	5944036
Total length (>= 5000 bp)	5787618	5822453	5917292
Total length (>= 10000 bp)	5746241	5795759	5902827
Total length (>= 25000 bp)	5681181	5640343	5842342
Total length (>= 50000 bp)	5467266	5390921	5734453
# contigs	133	105	43
Largest contig	752589	471587	1305359
Total length	5873426	5887191	5950746
GC (%)	35.13	35.18	35.18
N50	192084	206967	745621
N75	97805	127395	315452
L50	8	10	3
L75	18	20	6
# N's per 100 kbp	0.00	10.36	0.00

(D)

All statistics are based on contigs of size >= 500 bp, unless otherwise noted (e.g., "# contigs (>= 0 bp)" and "Total length (>= 0 bp)" include all contigs).

Figure S2: Quast report for SRB1 genome assembled with three different programs: Velvet, MaSuRCA and Spades. (A) shows the distribution of GC content in the contigs.; (B) shows the growth of contig lengths, contigs are ordered from the largest to smallest on the x-axis, while one the y-axis the size of the x largest contigs in the assemblies is depicted; (C) shows Nx values as x varies from 0 to 100 %, Nx is the length for which all the contigs with that set length or longer cover at least x% of the assembly; (D) shows the report where the three assemblies are compared.

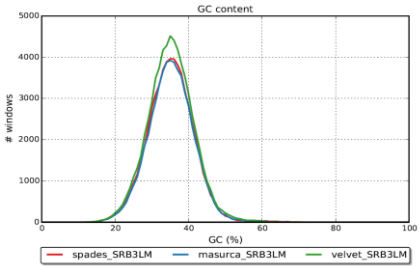

(A)

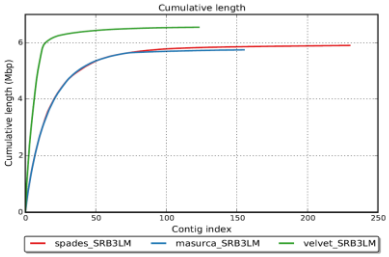

(B)

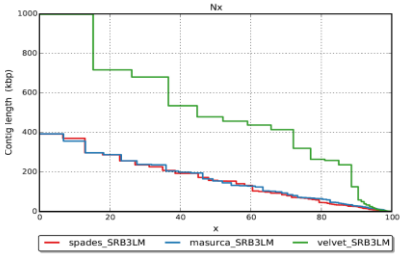

(C)

Report

	spades_SRB3LM	masurca_SRB3LM	velvet_SRB3LM
# contigs (>= 0 bp)	1066	183	123
# contigs (>= 1000 bp)	139	129	93
# contigs (>= 5000 bp)	86	74	42
# contigs (>= 10000 bp)	64	67	27
# contigs (>= 25000 bp)	49	46	19
# contigs (>= 50000 bp)	30	31	15
Total length (>= 0 bp)	6129103	5756772	6545436
Total length (>= 1000 bp)	5845725	5728078	6524375
Total length (>= 5000 bp)	5723357	5643076	6394304
Total length (>= 10000 bp)	5561013	5589579	6285968
Total length (>= 25000 bp)	5324575	5269841	6160389
Total length (>= 50000 bp)	4684963	4740540	6030343
# contigs	230	155	123
Largest contig	391991	392876	997779
Total length	5901766	5745734	6545436
GC (%)	35.15	35.23	35.13
N50	157736	154758	478895
N75	68944	70254	319746
L50	12	12	5
L75	26	25	9
# N's per 100 kbp	0.00	3.60	0.00

All statistics are based on contigs of size >= 500 bp, unless otherwise noted (e.g., "# contigs (>= 0 bp)" and "Total length (>= 0 bp)" include all contigs).

(D)

Figure S3: Quast report for SRB3 genome assembled with three different programs: Velvet, MaSuRCA and Spades. (A) shows the distribution of GC content in the contigs.; (B) shows the growth of contig lengths, contigs are ordered from the largest to smallest on the x-axis, while one the y-axis the size of the x largest contigs in the assemblies is depicted; (C) shows Nx values as x varies from 0 to 100 %, Nx is the length for which all the contigs with that set length or longer cover at least x% of the assembly; (D) shows the report where the three assemblies are compared.

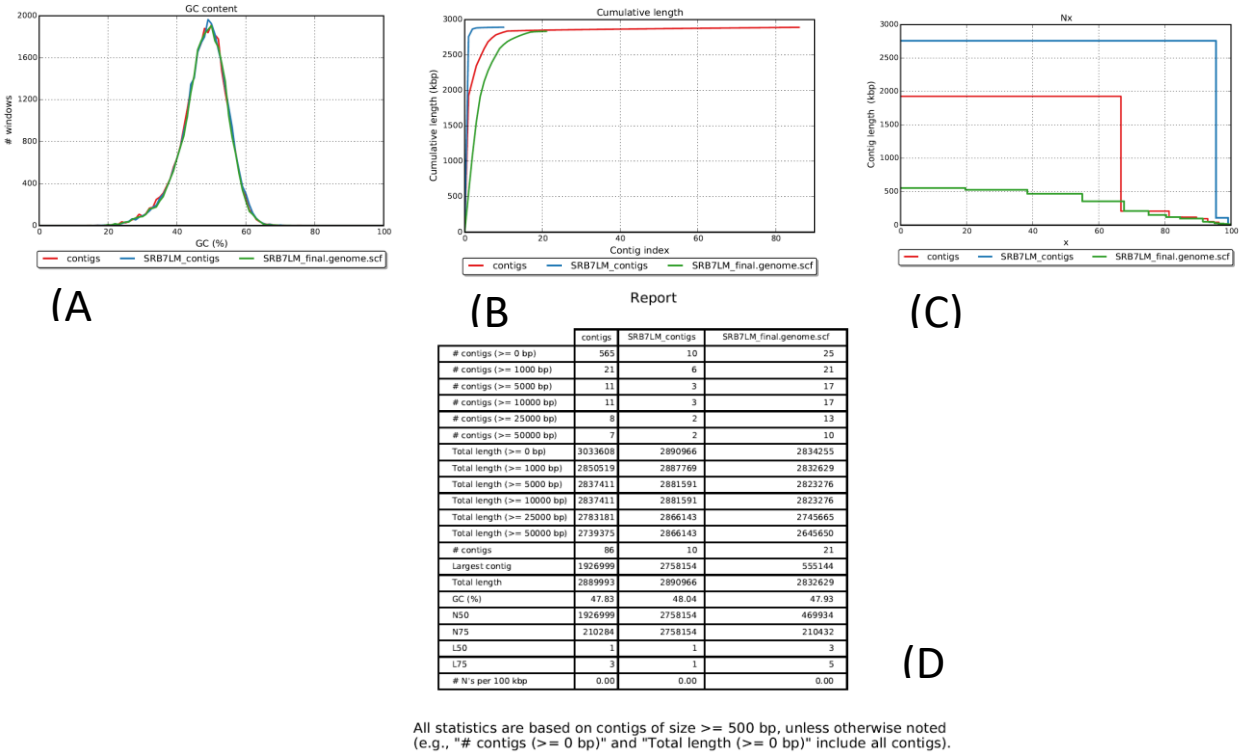

Report

	contigs	SRB7LM_contigs	SRB7LM_final.genome.scf
# contigs (>= 0 bp)	565	10	25
# contigs (>= 1000 bp)	21	6	21
# contigs (>= 5000 bp)	11	3	17
# contigs (>= 10000 bp)	11	3	17
# contigs (>= 25000 bp)	8	2	13
# contigs (>= 50000 bp)	7	2	10
Total length (>= 0 bp)	3033608	2890966	2834255
Total length (>= 1000 bp)	2850519	2887769	2832629
Total length (>= 5000 bp)	2837411	2881591	2823276
Total length (>= 10000 bp)	2837411	2881591	2823276
Total length (>= 25000 bp)	2783181	2866143	2745665
Total length (>= 50000 bp)	2739375	2866143	2645650
# contigs	86	10	21
Largest contig	1926999	2758154	555144
Total length	2889993	2890966	2832629
GC (%)	47.83	48.04	47.93
N50	1926999	2758154	469934
N75	210284	2758154	210432
L50	1	1	3
L75	3	1	5
# N's per 100 kbp	0.00	0.00	0.00

(D

All statistics are based on contigs of size >= 500 bp, unless otherwise noted (e.g., "# contigs (>= 0 bp)" and "Total length (>= 0 bp)" include all contigs).

Figure S4: Quast report for SRB7 genome assembled with three different programs: Velvet (SRB7LM_contigs), MaSuRCA (SRB7LM_final_genome_scf) and Spades (contigs). (A) shows the distribution of GC content in the contigs.; (B) shows the growth of contig lengths, contigs are ordered from the largest to smallest on the x-axis, while one the y-axis the size of the x largest contigs in the assemblies is depicted; (C) shows Nx values as x varies from 0 to 100 %, Nx is the length for which all the contigs with that set length or longer cover at least x% of the assembly; (D) shows the report where the three assemblies are compared.

Lineage of the isolates

Table S1: Lineage of each isolate.

	SRB1_LM	**SRB3_LM**	**SRB7_LM**
Domain	Bacteria	Bacteria	Bacteria
Phylum	Firmicutes	Firmicutes	Firmicutes
Class	Bacilli	Bacilli	Bacilli
Order	Bacillales	Bacillales	Bacillales
Family	Bacillaceae	Bacillaceae	Bacillales Family XII Incertae Sedis
Genus	*Bacillus*	*Bacillus*	*Exiguobacterium*
Species	*B. cereus*		

Growth rate calculations

To measure the growth rates, only the exponential phase needs to be considered and it varies from isolate to isolate and also within the same isolate it differs at different temperatures and different conditions (aerobic or anaerobic). By looking at each growth curve, the exponential phase at each condition was assessed and then the Ln(OD_{600nm}) of the time points in exponential phase was measured.

Then by plotting the time versus the Ln(OD), a straight line is obtained and the maximum growth rate (μ_{max}) at those specific conditions is given by the slope of the line.

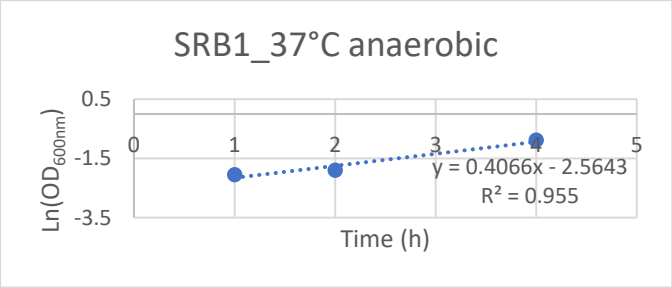

Figure S5: By looking at Figure 8 in the results section, the exp phase for SRB1LM at 37°C in anaerobic conditions was from time 1h to 4h. μ_{max} at these conditions is 0.4066 h^{-1}.

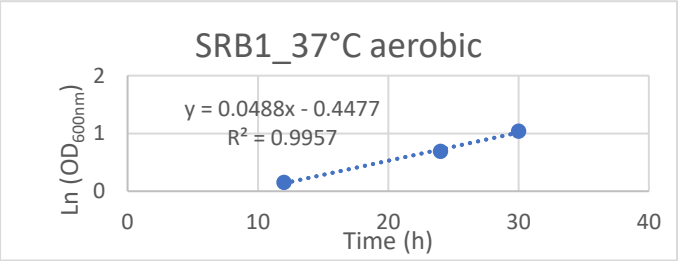

Figure S6: By looking at Figure 8 in the results section, the exp phase for SRB1LM at 37°C in aerobic conditions was from time 12h to 30h. μ_{max} at these conditions is 0.0488 h^{-1}.

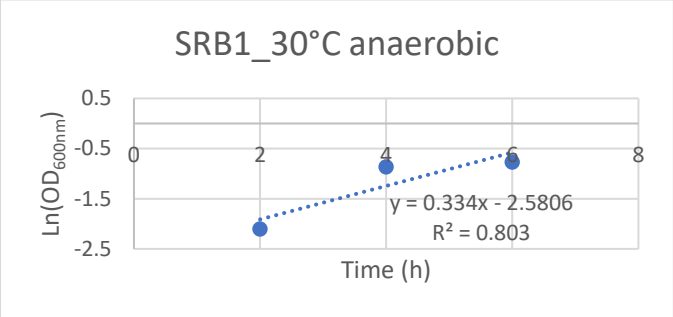

Figure S7: By looking at Figure 8 in the results section, the exp phase for SRB1LM at 30°C in anaerobic conditions was from time 2h to 6h. μ_{max} at these conditions is 0.334 h^{-1}.

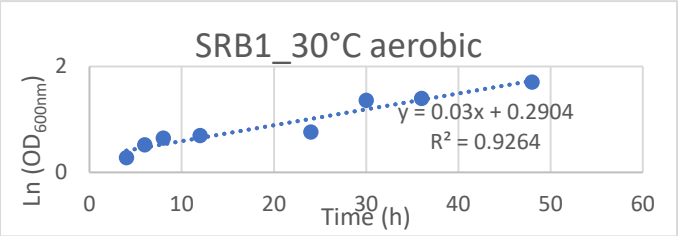

Figure S8: By looking at Figure 8 in the results section, the exp phase for SRB1LM at 30°C in aerobic conditions was from time 4h to 48h. μ_{max} at these conditions is 0.03 h^{-1}.

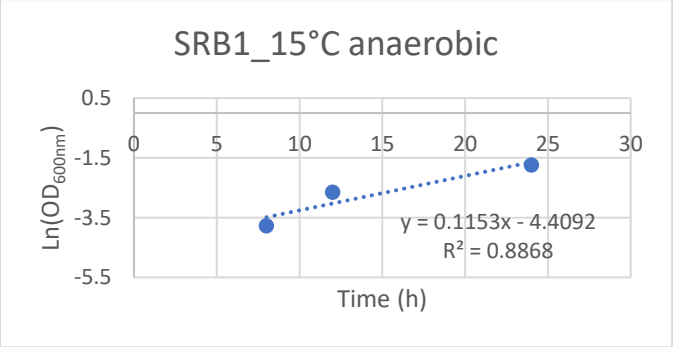

Figure S9: By looking at Figure 8 in the results section, the exp phase for SRB1LM at 15°C in anaerobic conditions was from time 8h to 24h. μ_{max} at these conditions is 0.1153 h^{-1}.

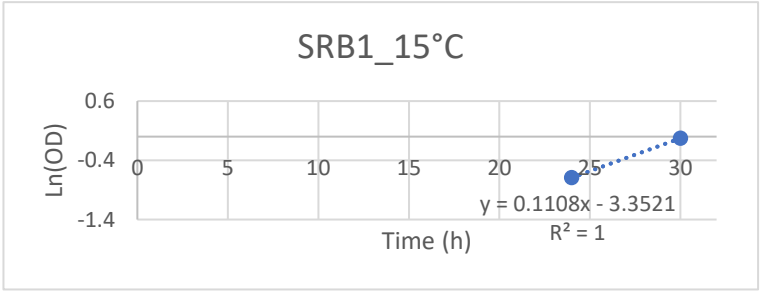

Figure S10: By looking at Figure 8 in the results section, the exp phase for SRB1LM at 15°C in aerobic conditions was from time 24h to 30h. μ_{max} at these conditions is 0.2645 h^{-1}.

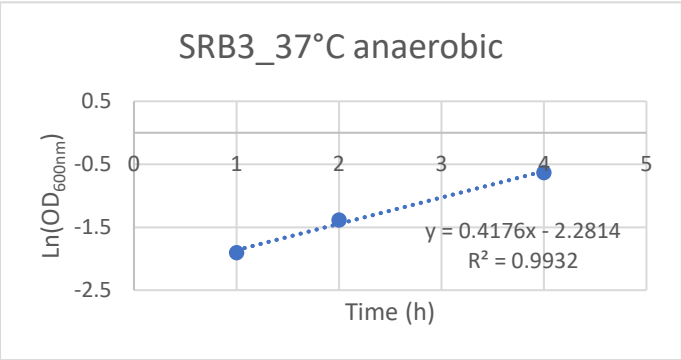

Figure S11: By looking at Figure 9 in the results section, the exp phase for SRB3LM at 37°C in anaerobic conditions was from time 1h to 4h. μ_{max} at these conditions is 0.4176 h^{-1}.

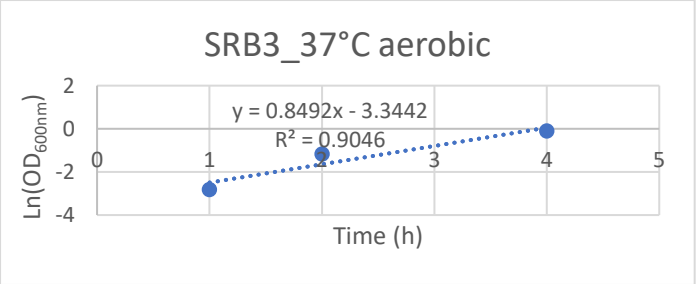

Figure S12: By looking at Figure 9 in the results section, the exp phase for SRB3LM at 37°C in aerobic conditions was from time 1h to 4h. μ_{max} at these conditions is 0.8492 h^{-1}.

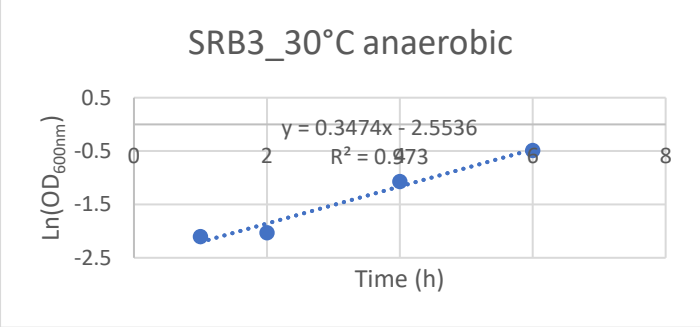

Figure S13: By looking at Figure 9 in the results section, the exp phase for SRB3LM at 30°C in anaerobic conditions was from time 1h to 6h. μ_{max} at these conditions is 0.3474 h^{-1}.

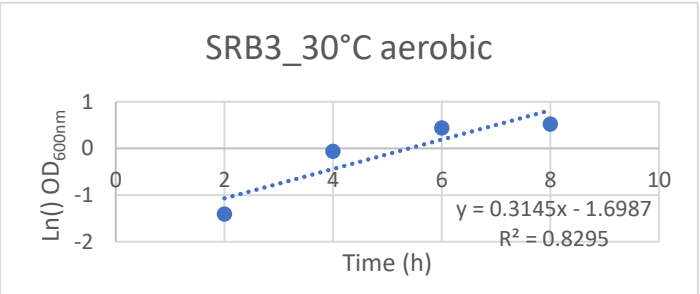

Figure S14: By looking at Figure 9 in the results section, the exp phase for SRB3LM at 30°C in aerobic conditions was from time 2h to 8h. μ_{max} at these conditions is 0.3145 h^{-1}.

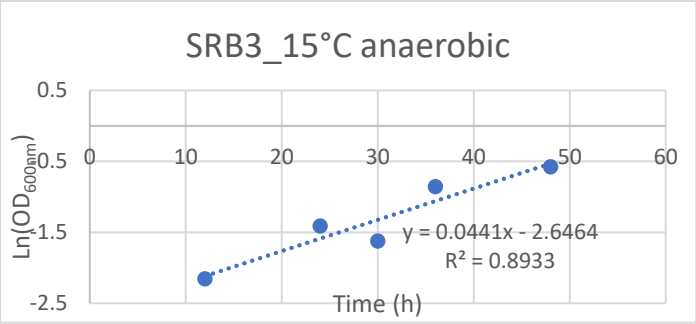

Figure S15: By looking at Figure 9 in the results section, the exp phase for SRB3LM at 15°C in anaerobic conditions was from time 12h to 48h. μ_{max} at these conditions is 0.0441 h^{-1}.

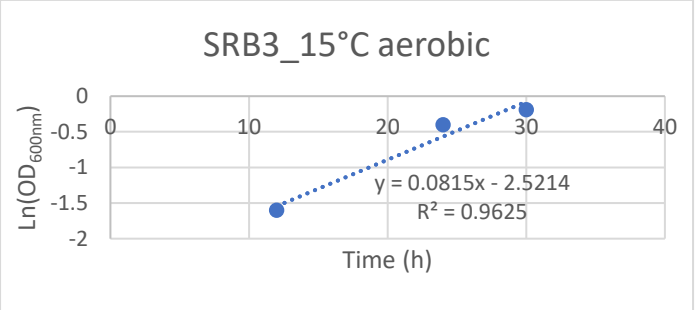

Figure S16: By looking at Figure 9 in the results section, the exp phase for SRB3LM at 15°C in aerobic conditions was from time 12h to 30h. μ_{max} at these conditions is 0.0815 h^{-1}.

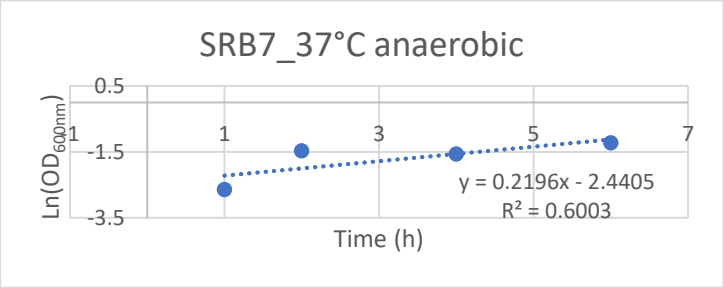

Figure S17: By looking at Figure 10 in the results section, the exp phase for SRB7LM at 37°C in anaerobic conditions was from time 1h to 6h. μ_{max} at these conditions is 0.2196 h^{-1}.

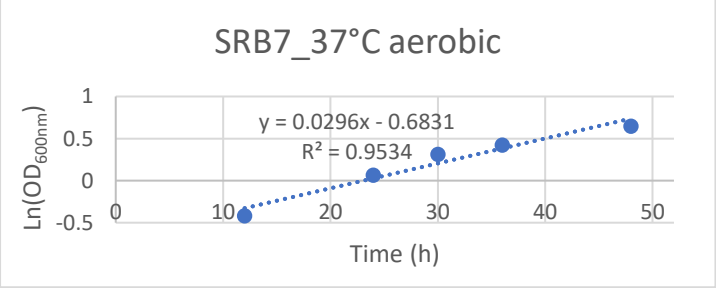

Figure S18: By looking at Figure 10 in the results section, the exp phase for SRB7LM at 37°C in aerobic conditions was from time 12h to 48h. μ_{max} at these conditions is 0.0296 h^{-1}.

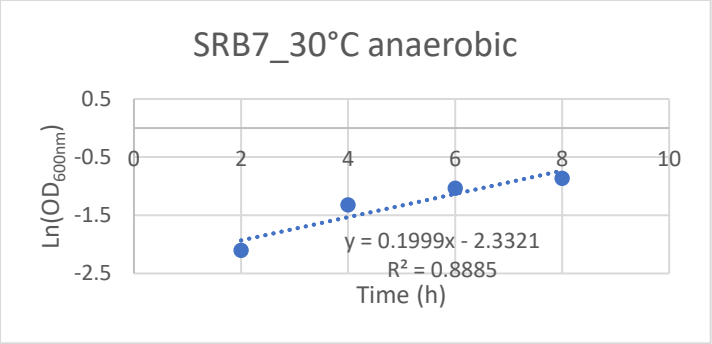

Figure S19: By looking at Figure 10 in the results section, the exp phase for SRB7LM at 30°C in anaerobic conditions was from time 2h to 8h. μ_{max} at these conditions is 0.1999 h^{-1}.

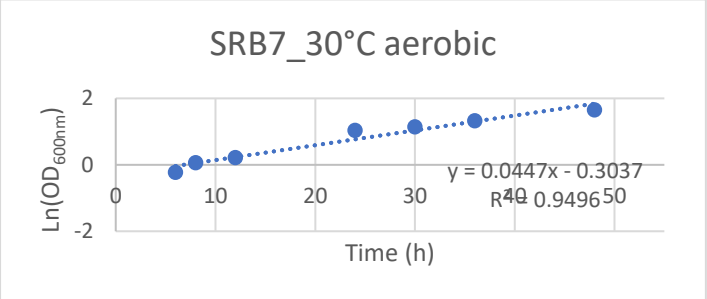

Figure S20: By looking at Figure 10 in the results section, the exp phase for SRB7LM at 30°C in aerobic conditions was from time 6h to 48h. μ_{max} at these conditions is 0.0447 h^{-1}.

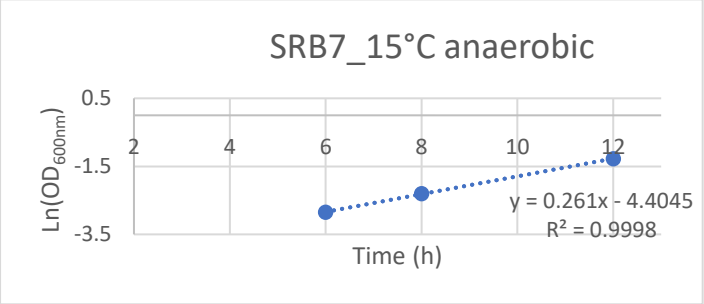

Figure S21: By looking at Figure 10 in the results section, the exp phase for SRB7LM at 15°C in anaerobic conditions was from time 6h to 12h. μ_{max} at these conditions is 0.261 h^{-1}.

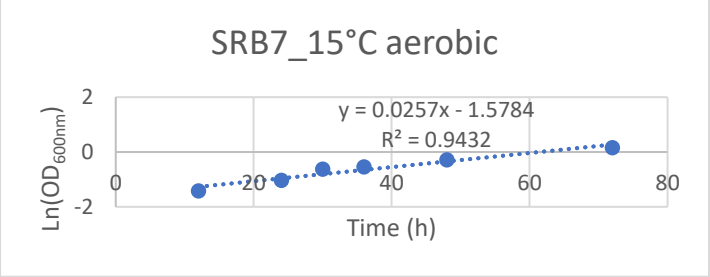

Figure S22: By looking at Figure 10 in the results section, the exp phase for SRB7LM at 15°C in aerobic conditions was from time 12h to 72h. μ_{max} at these conditions is 0.0257 h^{-1}.

PHB plates

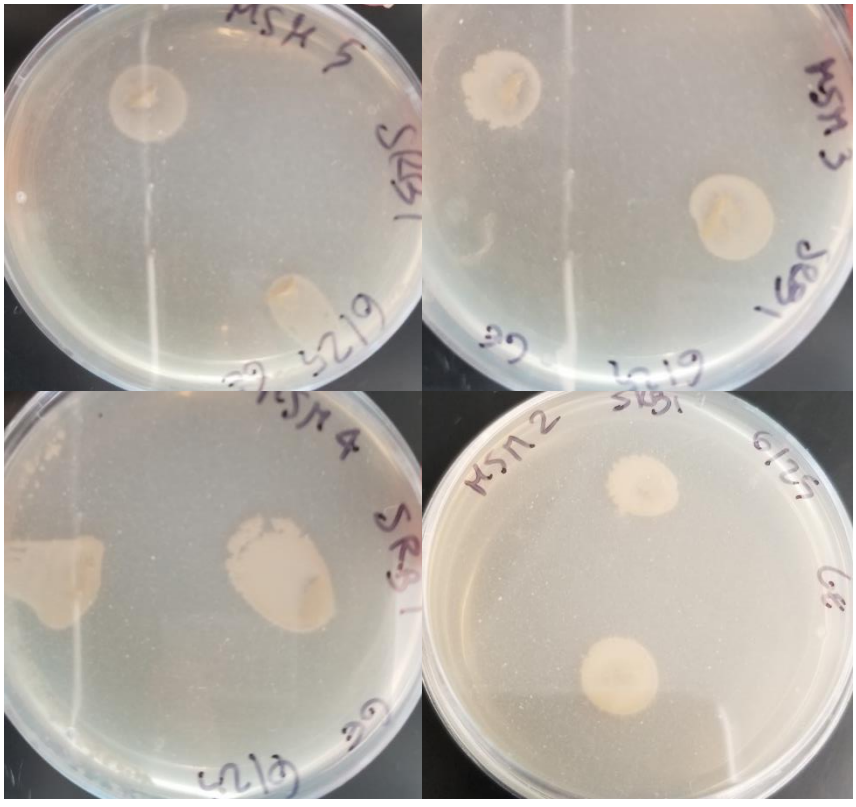

Figure S23: Plates with a bottom layer of MSM and a top layer of PHB 0.1%. SRB1LM was inoculated and incubated at 37°C. Pictures were then taken after 5 days of incubation and colonies can be seen.

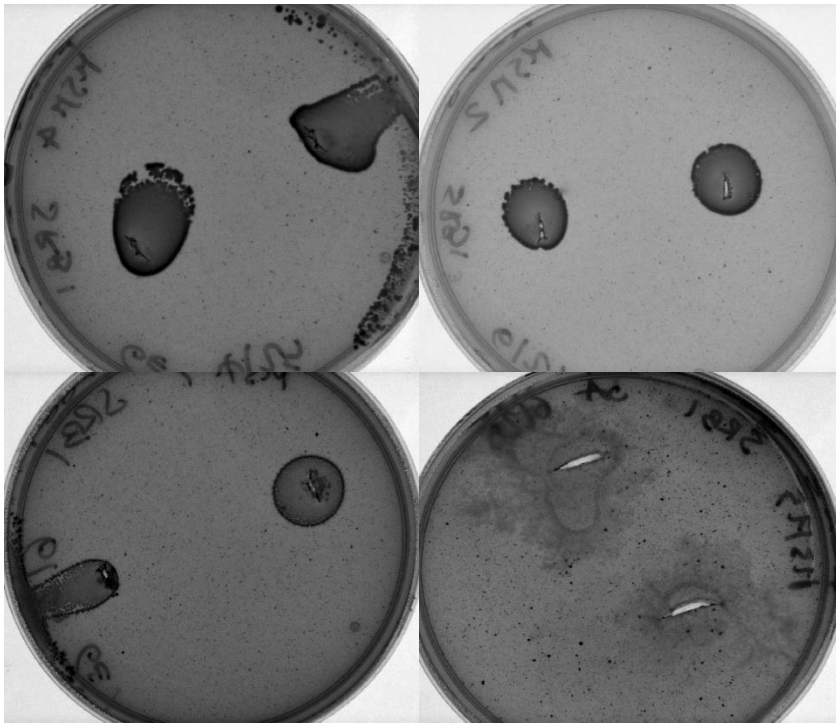

Figure S24: Plates with a bottom layer of MSM and a top layer of PHB 0.1%. SRB1LM was inoculated and incubated at 37°C. Pictures with a Bio-Rad gel imager were then taken after 5 days of incubation and colonies can be seen.

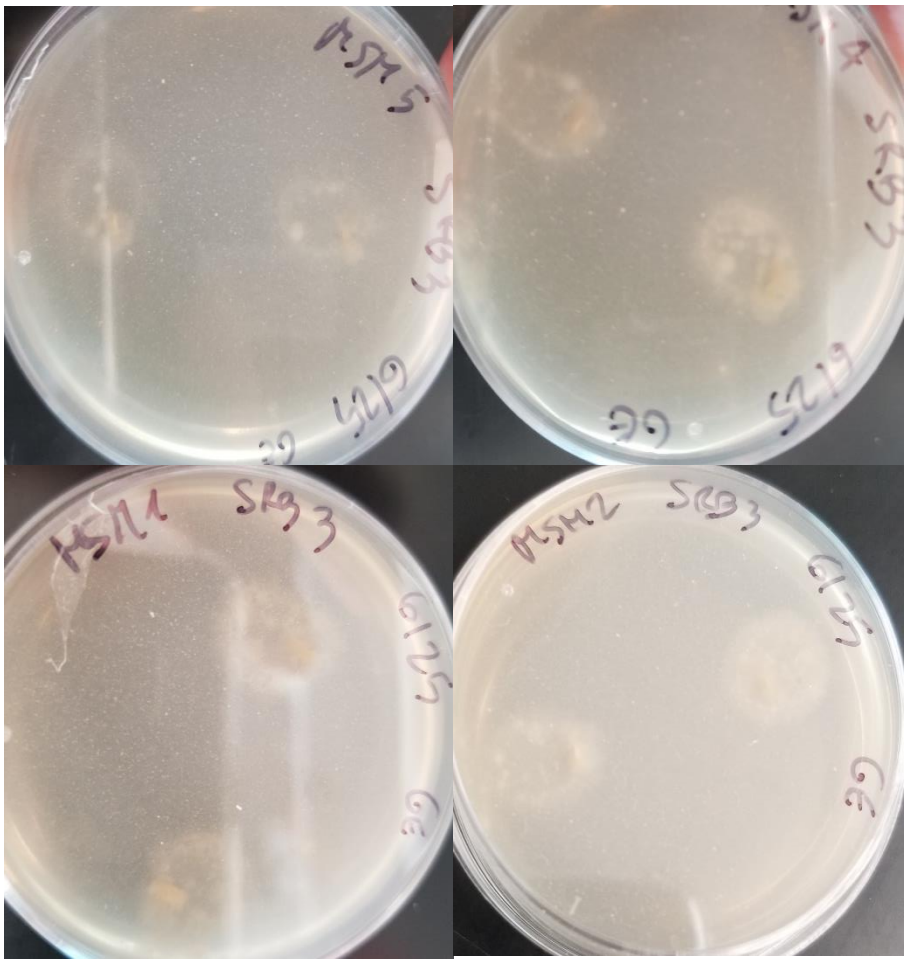

Figure S25: Plates with a bottom layer of MSM and a top layer of PHB 0.1%. SRB3LM was inoculated and incubated at 37°C. Pictures were then taken after 5 days of incubation and colonies can be seen.

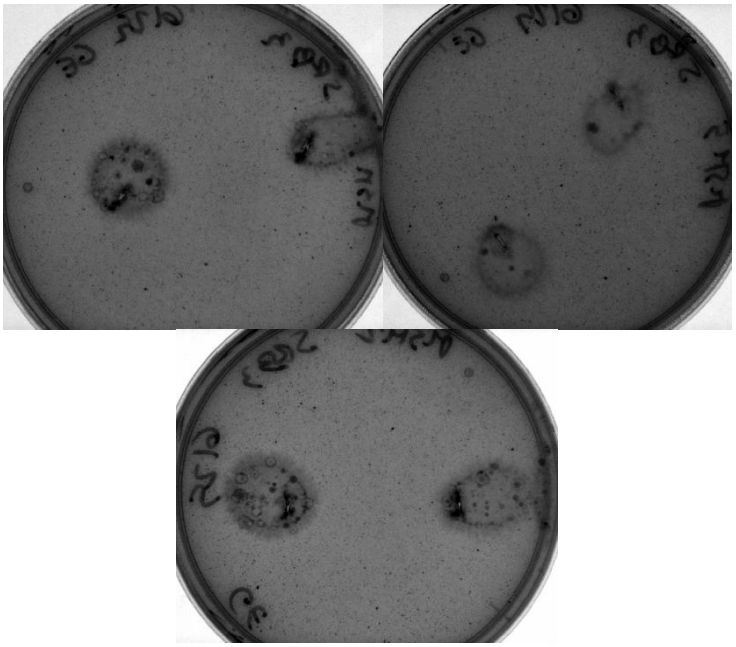

Figure S26: Plates with a bottom layer of MSM and a top layer of PHB 0.1%. SRB1LM was inoculated and incubated at 37°C. Pictures with a Bio-Rad gel imager were then taken after 5 days of incubation and colonies can be seen.

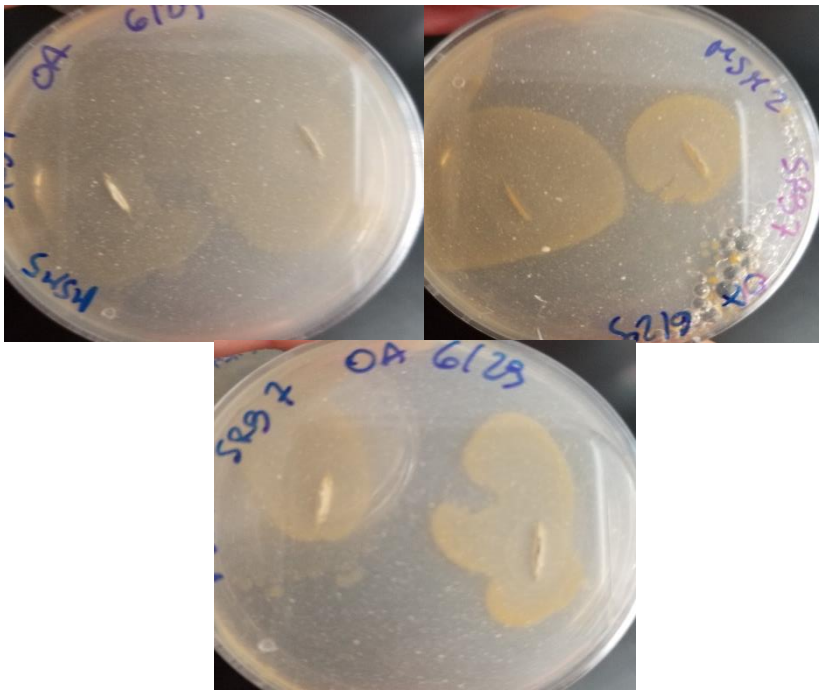

Figure S27: Plates with a bottom layer of MSM+oxyrase and a top layer of PHB 0.1%. SRB7LM was inoculated and incubated at 37°C. Pictures were then taken after 5 days of incubation and colonies can be seen.

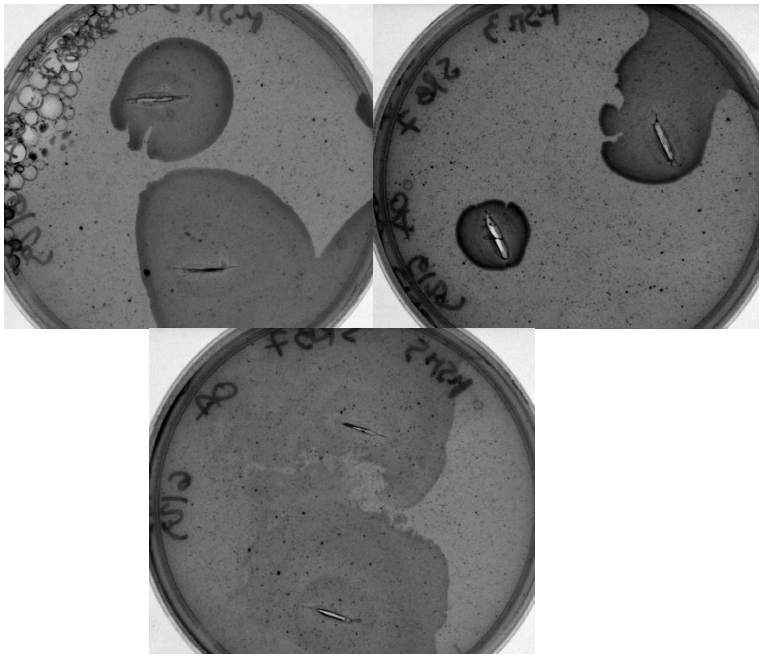

Figure S28: Plates with a bottom layer of MSM and a top layer of PHB 0.1%. SRB7LM was inoculated and incubated at 37°C. Pictures with a Bio-Rad gel imager were then taken after 5 days of incubation and colonies can be seen.

Maximum-likelihood trees

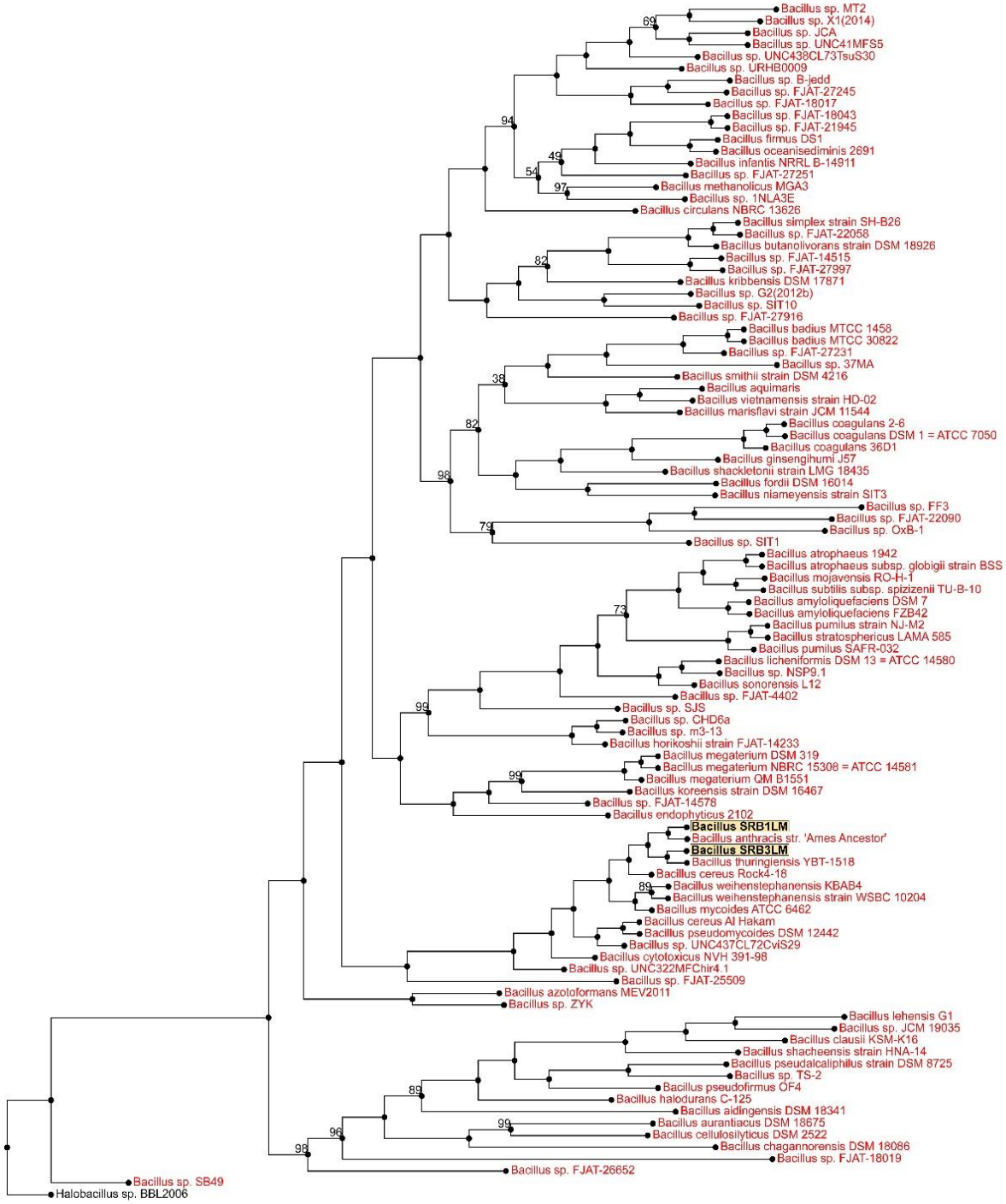

Figure S29: Maximum-likelihood phylogenetic tree based on PATRIC's comprehensive genome analysis service. 98 genomes within *Bacillus* in the PATRIC database were included in the tree. The position of isolates SRB1LM and SRB3LM is highlighted in yellow.Node labels show the bootstrap support values, and values of 100% are not shown. Branch lengths represent the average number of substitutions per site. The tree was rooted to a more distantly related *Bacillaceae* (*Halobacillus sp.* BBL2006).

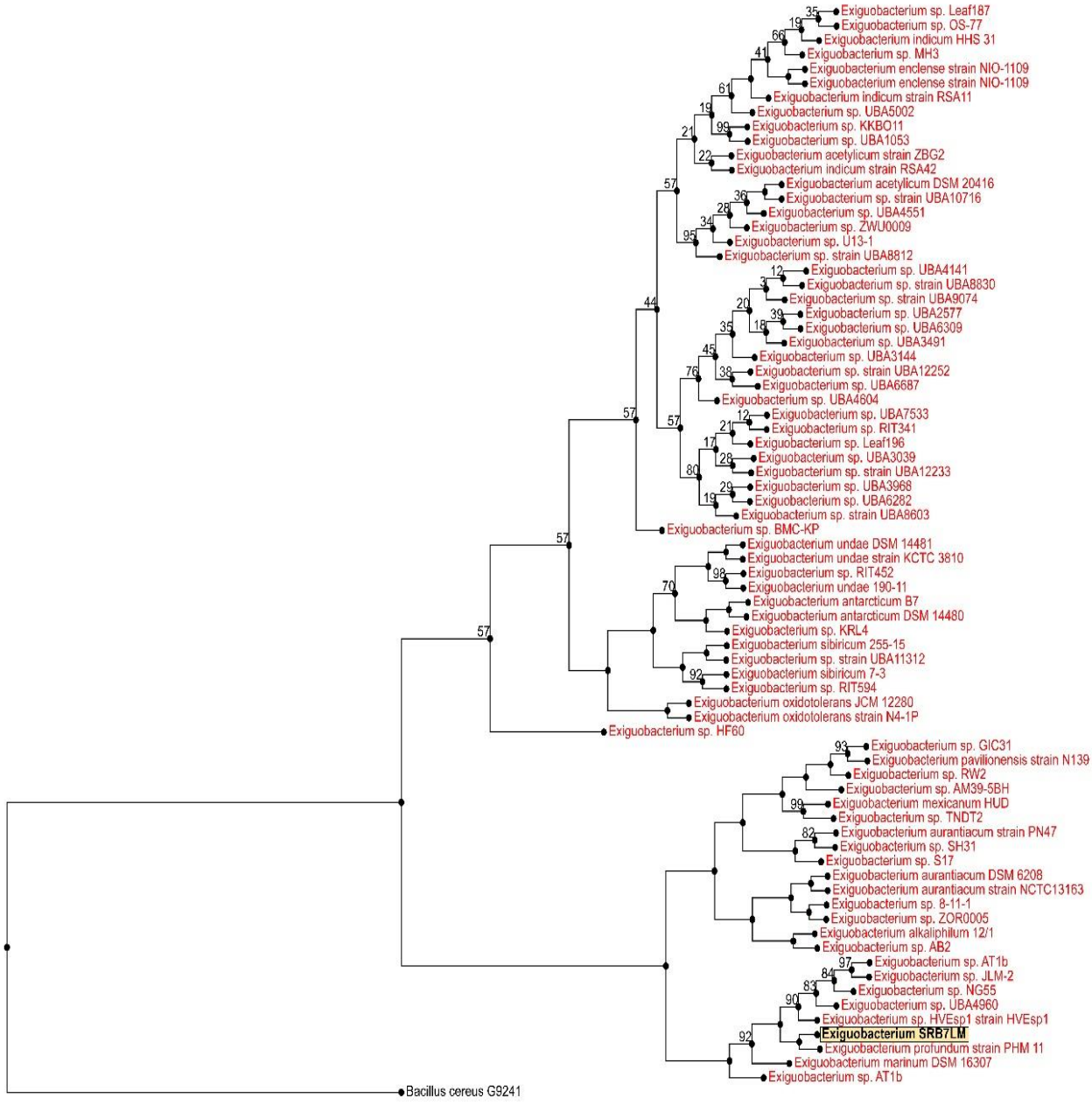

Figure S30: Maximum-likelihood phylogenetic tree based on PATRIC's comprehensive genome analysis service. 75 genomes within *Exiguobacterium* in the PATRIC database were included in the tree. The position of isolate SRB7LM is highlighted in yellow.Node labels show the bootstrap support values, and values of 100% are not shown. Branch lengths represent the average number of substitutions per site. The tree was rooted to a more distantly related *Bacillaceae* (*Bacillus cereus* G9241).